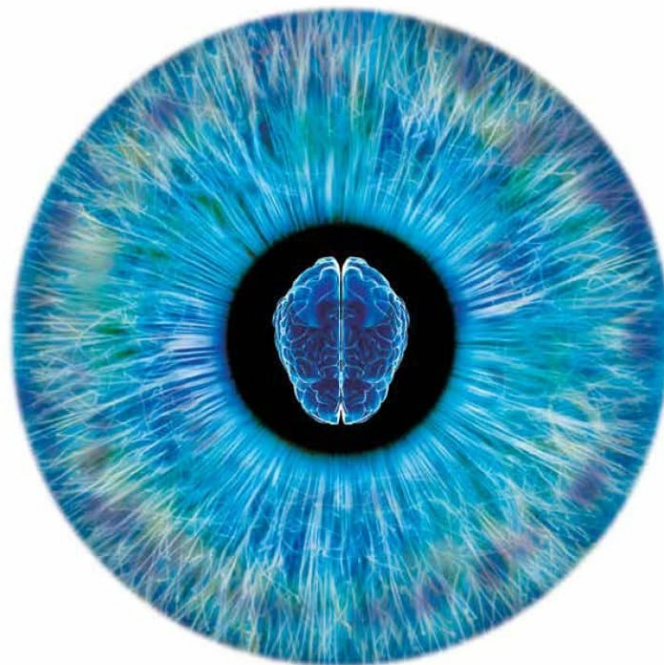


Diploma thesis

Multi-Wavelength Dynamic Imaging of the Pupillary Photomotor Reflex

Karimpidis Dionisios



Committee:

Professor Balas Constantinos (Supervisor)

Professor Kalaitzakis Constantinos

Associate professor Bucher Mattias

Technical University of Crete

Chania January 2018

Multi-Wavelength Dynamic Imaging of the Pupillary Photomotor Reflex

Abstract

Pupillography is utilized as a method in order to record changes of the pupil diameter. Nervous System and especially Autonomic Nervous System (ANS) is responsible for controlling pupil reflexes, hence the pupil changes occur subconsciously. In this study an innovative, low-cost and wireless imaging system device developed for pupil non-invasive examination. The device is portable and there is also a possibility to apply different light stimulus within the visible spectrum and analyze the behavior of the pupil reaction. The goal of this thesis is to provide the proper device instrumentation and a basic algorithmic method to measure reliably and objectively the pupil diameter. For the needs of the proposed system an image processing algorithm and a graphic user interface was developed to control the device wirelessly. Due to the relation of pupillary reflexes and ANS, digital pupillography presents a simple and real time window for its functionality. Pupil responses may associate with a various pathologies such as brain or mental diseases, anxiety or autism with an uprising research interest from various clinical studies to psychological impacting conditions.

Table of Contents

Figures List.....	4
Chapter1: Biological View.....	6
1.1 Human eye anatomy.....	6
1.2 Nervous System.....	7
1.2.1 Sympathetic Nervous System.....	8
1.2.2 Parasympathetic Nervous System.....	9
1.3 Pupillary light reflex.....	10
1.3.1 Iris sphincter and miosis	10
1.3.2 Iris dilator and mydriasis.....	10
1.3.3 pupil constriction neural circuit.....	11
1.3.4 pupil dilation neural circuit.....	12
1.4 multicolor eye excitation.....	12
1.4.1 Rod cells.....	13
1.4.2 Cone cells.....	13
1.4.3 Vision Regimes.....	14
Chapter2: Pupillography till today.....	16
2.1 Introduction.....	16
2.2 application on diseases	16
2.2.1 Eye diseases	16
2.2.2 Pupillography in psychology	17
2.2.3 Drugs and pharmaceuticals	17
2.2.4 Diabetes and Cardiovascular Neuropathy	18
2.2.5 Brain and mental disorders	18
2.2.6 Psychiatric disorders and anxiety	18
2.2.7 Alternative Cures.....	19
2.3 Pupillography devices.....	19
2.4 Statement of purpose.....	22
Chapter 3: Device instrumentation.....	23
3.1 Virtual reality mask.....	24
3.2 Raspberry pi zero wifi.....	24
3.3 Raspberry camera module.....	25
3.4 Arduino nano	25
3.5 TLC5940 microcontroller.....	26
3.6 Leds and resistors	26
3.7 Batteries, charger, converter, monitor and a switch.....	33
Chapter4: Software Development.....	36
4.1 LEDs Driving Procedure.....	36
4.2 Qt GUI and layout.....	37
4.3 Pupil measurement algorithm.....	40
Conclusion and future work.....	43
References.....	44

Figures List

Figure 1.1: Human eye

Figure 1.2: Divisions of Nervous System

Figure 1.3: Sympathetic Nervous System pathways

Figure 1.4: Parasympathetic Nervous System pathways

Figure 1.5: sphincter and dilator muscles

Figure 1.6: Pupil constriction neural circuit

Figure 1.7: Pupil dilation neural circuit

Figure 1.8: light pathway through eye

Figure 1.9: rods and cones density

Figure 1.10: Difference in the level of convergence between rods and cones

Figure 1.11: relevant receptors to each of the regimes

Figure 2.1: Figure VIP-300 pupillometer

Figure 2.2: DP- 2000 Binocular Pupillometer

Figure 2.3: RAPDx pupillometer

Figure 2.4 (a) : Prototype experimental model

Figure 2.4 (b): Prototype experimental model

Figure 2.5 (a): experimental developed mask

Figure 2.5 (b): experimental developed mask

Figure 3.1: Schematic block diagram of all components

Figure 3.2: VR mask

Figure 3.3: raspberry Pi Zero Wifi

Figure 3.4: raspberry camera

Figure 3.5: arduino nano

Figure 3.6: TLC5940 microcontroller

Figure 3.7: rechargeable batteries

Figure 3.8: battery monitor

Figure 3.9: battery converter

Figure 3.10: battery charger

Figure 3.11: PCB wiring diagram

Figure 3.12: PCB front view

Figure 3.13: PCB rear view

Figure 3.14: Schematic block diagram of all components

Figure 4.1: LEDs functionality control

Figure 4.2: LEDs control algorithmic procedure

Figure 4.3: GUI layout to adjust program parameters

Figure 4.4: time steps

Figure 4.5: PLR test flow diagram

Figure 4.6: Patient Info page

Figure 4.7: Pupil measurement algorithmic steps

Figure 4.8 (a): original image

Figure 4.8 (b): inverted image

Figure 4.8 (c): binary image

Figure 4.8 (d): Pupil localization image

Figure 4.9: Puppilogram

Chapter1: Biological view

1.1 Human eye anatomy

Over the years many different animal vision systems have been observed, each perfectly tailored to suit the needs of its owner. Two of the most common types of eyes found in nature are the camera-type eye and compound eyes. The human eye is an example of a camera-type eye, which uses a single lens to focus images onto a light sensitive membrane lining the inside of the eyeball called the retina. Considering that the task of providing vision is really difficult it could be easily be understood that there are so many working parts

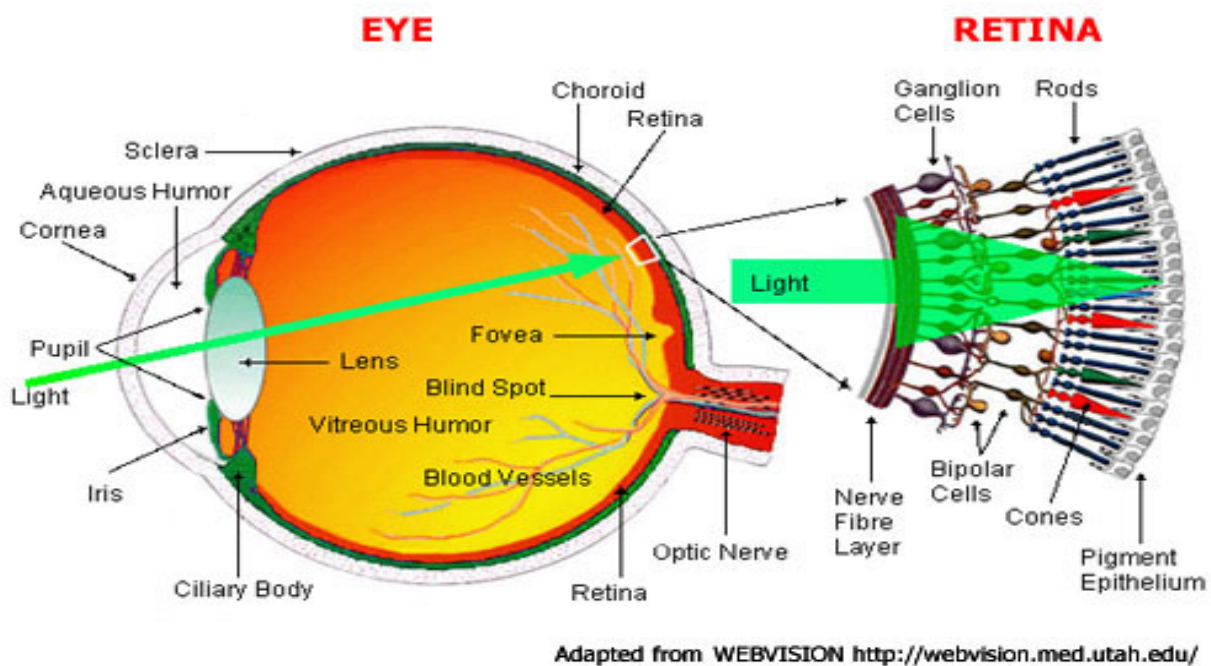


Figure 1.1: Human eye

Light is focused primarily by the **cornea** — the clear front surface of the eye, which acts like a **camera lens**.

The **iris** of the eye functions like the **diaphragm** of a camera, controlling the amount of light reaching the back of the eye by automatically adjusting the size of the pupil (aperture).

The eye's **crystalline lens** is located directly behind the pupil and further focuses light. Through a process called accommodation, this lens helps the eye automatically focus on near and approaching objects, like an **autofocus camera lens**.

Light focused by the cornea and crystalline lens (and limited by the iris and pupil) then reaches the **retina** — the light-sensitive inner lining of the back of the eye. The retina acts like an **electronic image sensor** of a digital camera, converting optical images into chemical and electronic signals. The optic nerve then transmits these signals to the visual cortex — the part of the brain that controls our sense of sight

Since this study is mainly oriented on pupil responses, its main functions are mentioned below. The pupil is the opening through which light enters the eye, regulating the amount of entering light. It also improves the visual acuity because it prevents the irregular refraction by the periphery of the cornea and lens, and increases the depth of focus. Finally it allows passage of aqueous humor from the posterior chamber to the anterior chamber.

1.2 Nervous System

The nervous system transmits signals to and from different parts of its body and it's consists of two main parts, the central nervous system (CNS) and the peripheral nervous system (PNS).

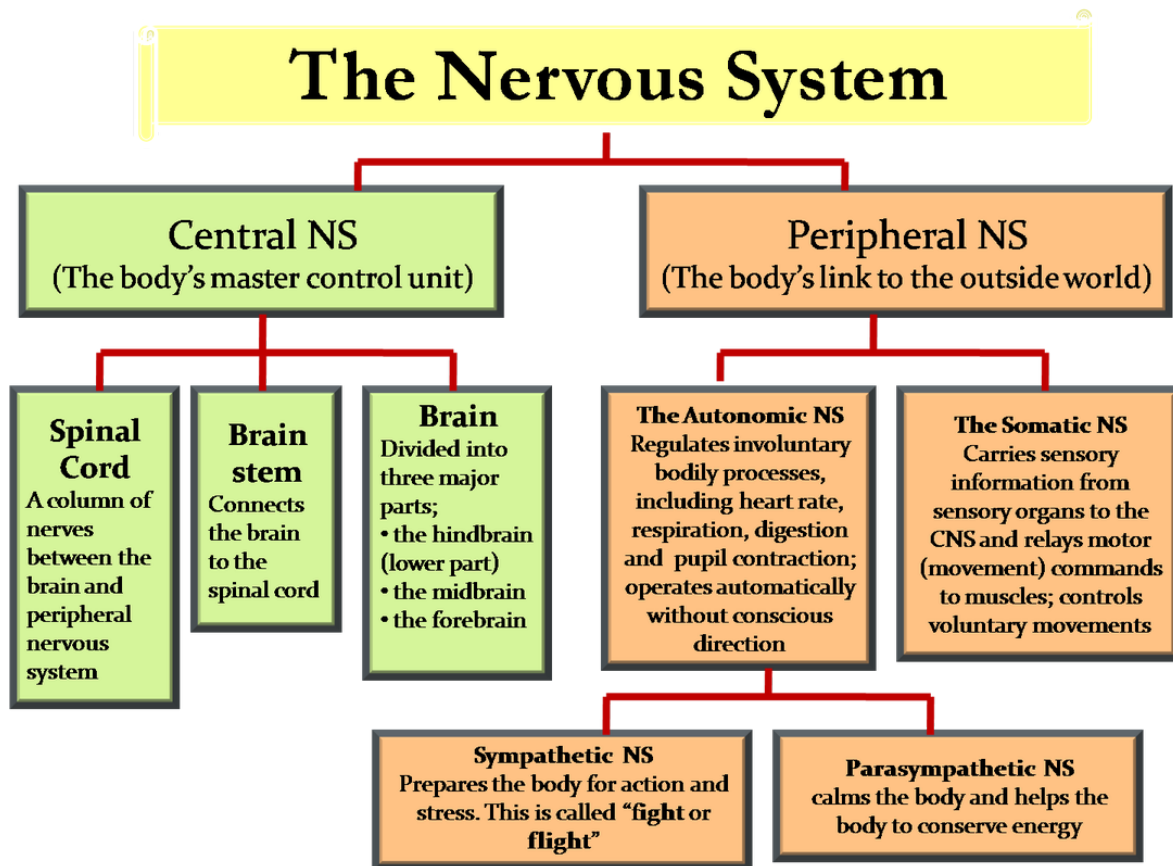


Figure 1.2: Divisions of Nervous System

The CNS consists of the brain, the spinal cord and the brain stem that connects these two parts. The PNS is the body's link to the outside word and consists mainly of nerves that connects the CNS to every other part of the body. Analyzing further, the PNS is divided into Autonomic Nervous System (ANS) responsible for the involuntary functions of the human body and Somatic Nervous System (SNS) responsible for the voluntary functions. Two parts of the ANS are examined further on this study. The Sympathetic Nervous System (SNS) and the Parasympathetic Nervous System (PSNS).

1.2.1 Sympathetic Nervous System

Sympathetic Nervous System controls the body's responses to a perceived threat and is responsible for the "fight or flight" response. Like other parts of the nervous system, the SNS operates through a series of interconnected neurons. Through it, there are two kinds of neurons, involved in the transmission of any signal. The preganglionic neurons which are relatively short and stem from the thoracolumbar region of spinal cord and postganglionic neurons that extend across most of the body. Within the ganglia, spinal cord sympathetic neurons join peripheral sympathetic neurons through chemical synapses. The sympathetic neuron pathway is composed from very short neurons so it's a faster system.

Fight-or-flight responses include:

- release of adrenaline from the adrenal gland
- increase in the heart rate
- contraction of muscles
- decrease in urinary output
- dilation of bronchial tubes in the lungs
- dilation of pupils in the eyes
- sphincter contraction

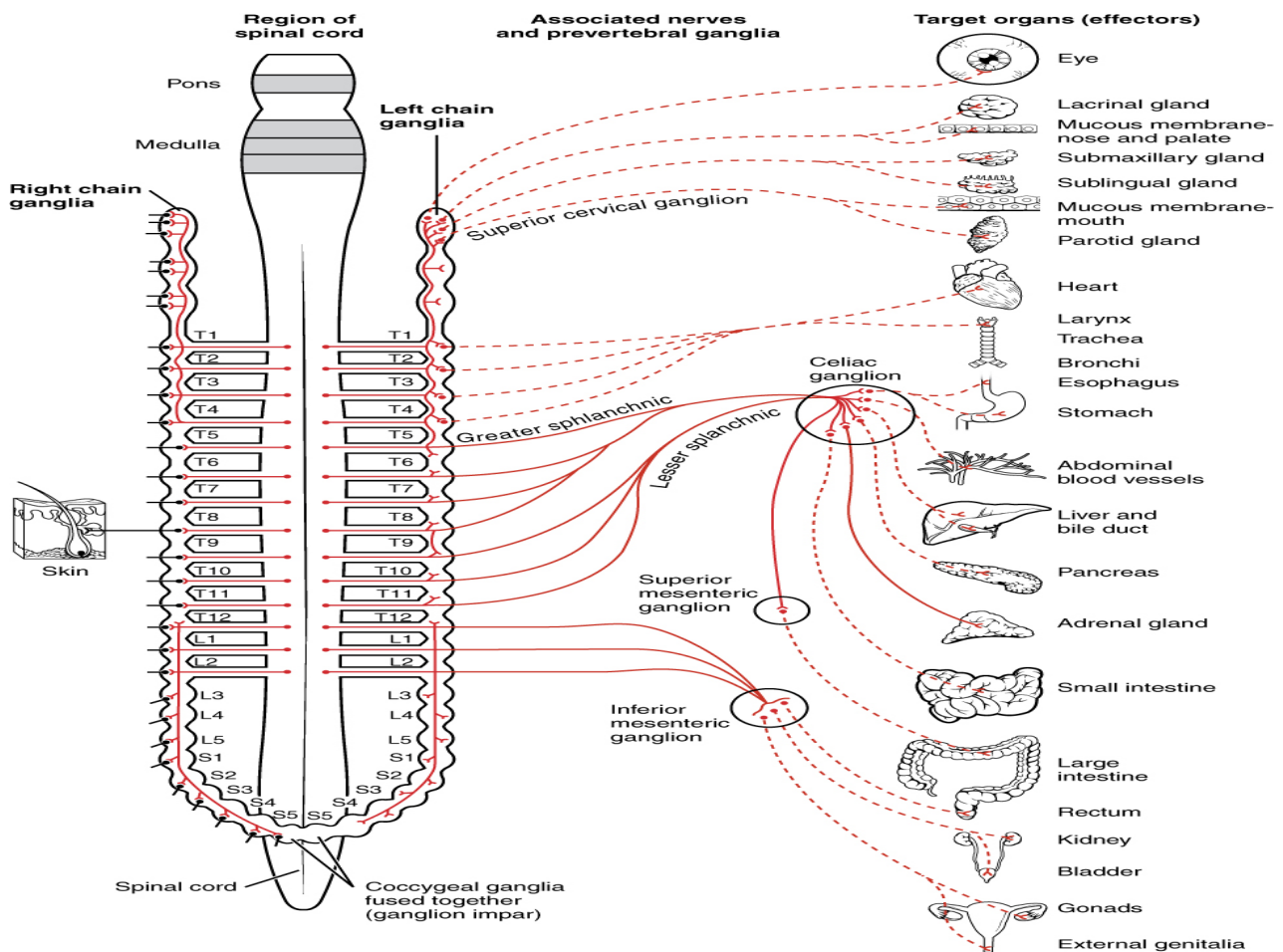


Figure 1.3: Sympathetic Nervous System pathways

1.2.2 Parasympathetic Nervous System

Parasympathetic Nervous System controls homeostasis and the body at rest and is responsible for the body's "rest and digest" function. PSNS restores the body to a state of calm and its action is described as being complementary to that of the SNS. Is commonly referred to as having "craniosacral outflow" instead of "thoracolumbar outflow" of SNS. The parasympathetic neuron pathway is composed from longer neurons so it's a slower system. In correspondence with SNS the PSNS:

- inhibits heart rate
- relaxes the muscles
- stimulates salivation
- stimulates digestive activity
- increases urinary output
- constricts bronchial tubes in the lungs
- constricts pupils in the eye
- relaxes the sphincter

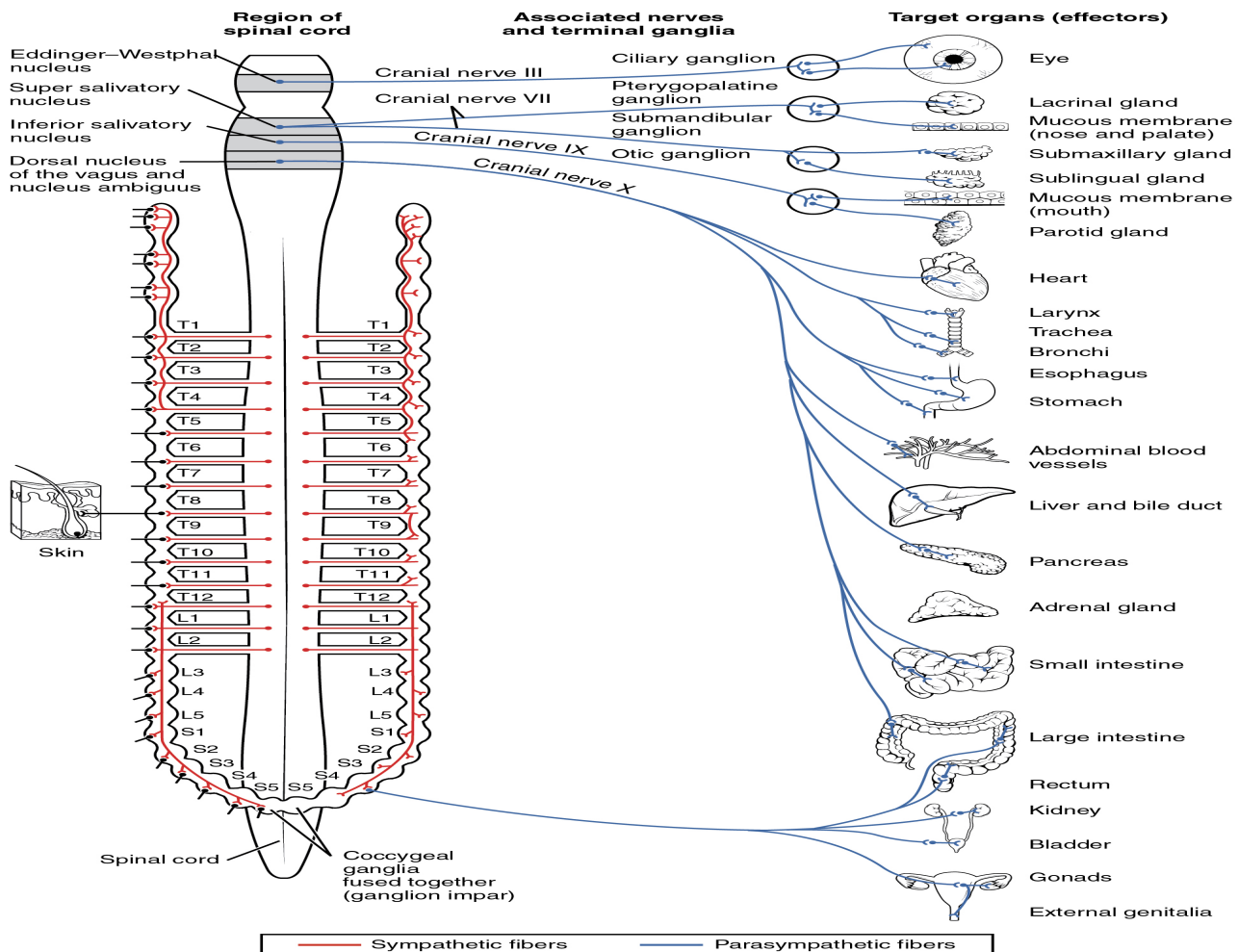


Figure 1.4: Parasympathetic Nervous System pathways

1.3 Pupillary light reflex

The pupillary light reflex (PLR) involves adjustments in pupil size with changes in light levels. A greater intensity of light constricts pupil allowing less light in whereas a lower intensity dilates pupil allowing more light in. The reflex is consensual: normally light that is directed in one eye produces pupil constriction in both eyes. The direct response is the change in pupil size in the eye to which the light is directed. The consensual response is the change in pupil size in the opposite eye to which the light is directed. Iris area is composed of two muscles, sphincter and dilator as shown in the image below.

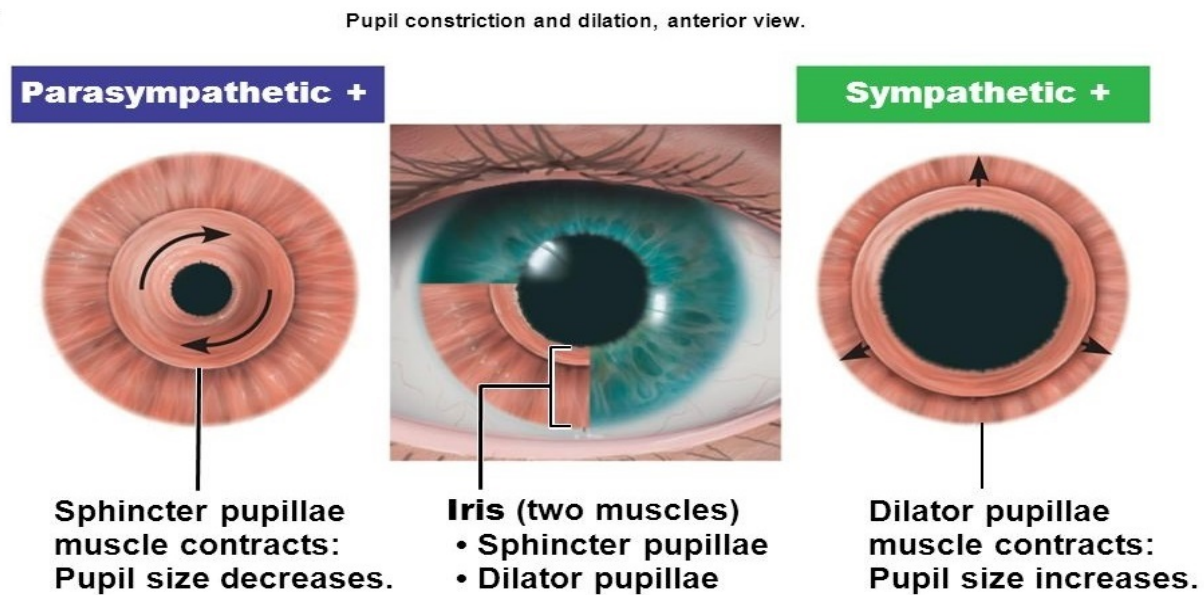


Figure 1.5: sphincter and dilator muscles

1.3.1 Iris sphincter and miosis

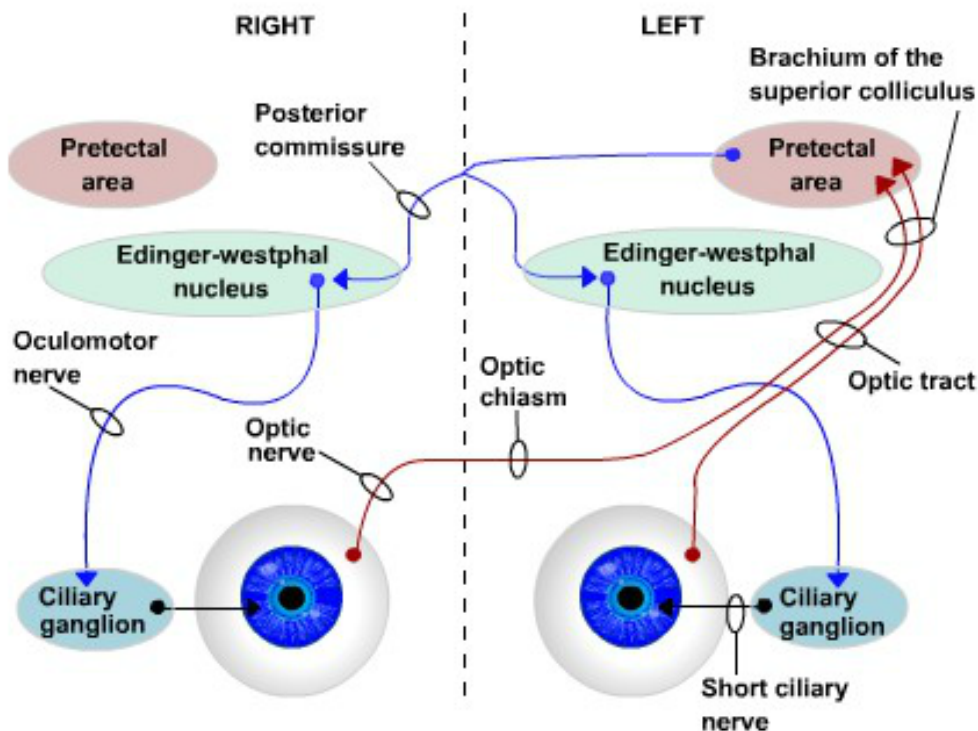
Iris sphincter is responsible for constriction called miosis and is part of PSNS. The sphincter muscle fibers form a ring at the pupil margin so that when the sphincter contracts, it decreases (constricts) pupil size. Miosis is a normal reaction to a light increase but it could be also associated with certain pathological conditions, drug use or microwave radiation exposure.

1.3.2 Iris dilator and mydriasis

On the other hand iris dilator is responsible for pupil dilation, called mydriasis and is part of SNS. The dilator muscle fibers radiate from the pupil aperture so that when the dilator contracts, it increases (dilates) pupil size. Mydriasis is a normal response on light decrease to improve visibility but as a non-physiological cause could indicate a disease, trauma or the use of drugs. The action of the dilator is antagonistic to that of the sphincter and the dilator must relax to allow the sphincter to decrease pupil size. Both muscles act to control the amount of entering light and the depth of field of the eye.

1.3.3 Pupil constriction neural circuit

Further examination of the pathway controlling pupil constriction neural circuit includes retina, optic nerve, optic chiasm, and the optic tract fibers that join the brachium of the superior colliculus, which terminate in the pretectal area of the midbrain. Pretectal nucleus sends most of its axons bilaterally in the posterior commissure to terminate in the Edinger-Westphal nucleus of the oculomotor complex, which contains parasympathetic preganglionic neurons. Its axons are sent in the oculomotor nerve to terminate in the ciliary ganglion, which sends its parasympathetic postganglionic axons in the short ciliary nerve, which ends on the iris sphincter.



The lines ending with an arrow indicate axons terminating in the structure at the tip of the arrow.

The lines beginning with a dot indicate axons originating in the structure containing the dot.

Figure 1.6: Pupil constriction neural circuit

As it was described above the PLR is consensual. This phenomenon occurs because the optical signal from the pretectal nucleus of pretectal area is transmitted to right and left Edinger-westphal nucleus so both ciliary ganglion are activated and both pupils react.

1.3.4 Pupil dilation neural circuit

The pathway controlling pupil dilation neural circuit includes retina and the optic tract fibers terminating on neurons in the hypothalamus and the axons of the hypothalamic neurons that descend to the spinal cord to end on the sympathetic preganglionic neurons in the lateral horn of spinal cord segments T1 to T3, which send their axons out the spinal cord to end on the sympathetic neurons in the superior cervical ganglion, which send their sympathetic postganglionic axons in the long ciliary nerve to the iris dilator.

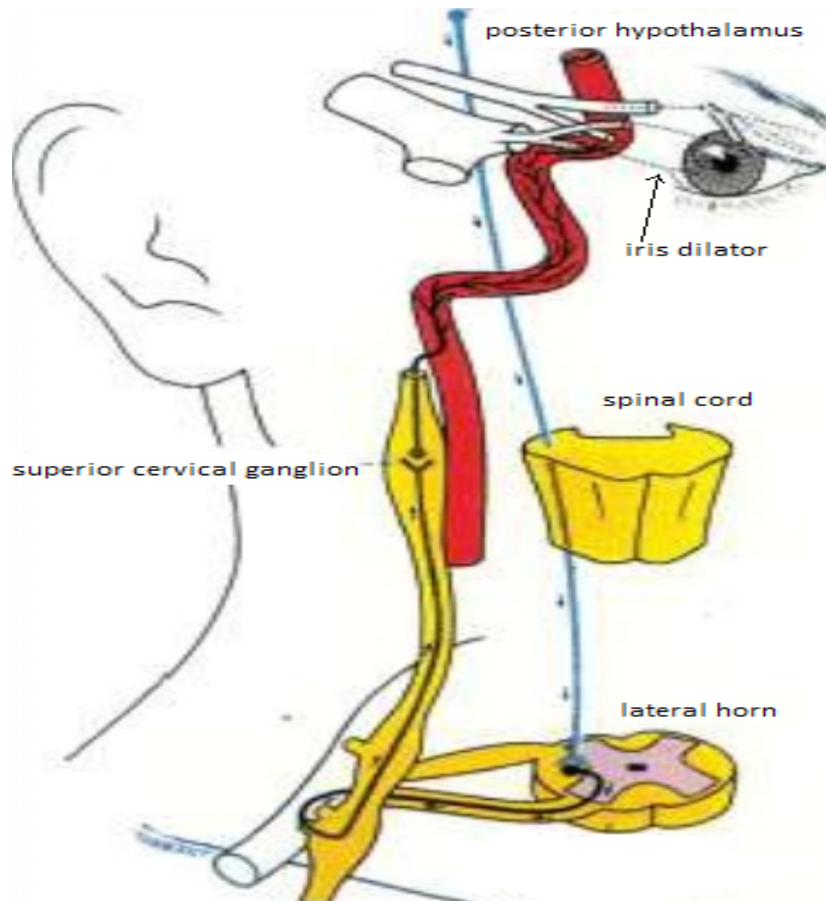


Figure 1.7: Pupil dilation neural circuit

1.4 Multicolor eye excitation

As discussed earlier retina is a thin layer of tissue that lines on the back of inner side of eye. There are different types of cell that are located in this region like light-sensitive rods and cones cells that convert incoming light into nerve signals, which are transmitted by the other retinal cells (ganglionic cells, bipolar cells, etc) to the optic nerve and from there to the brain. Light is passing through the retinal “circuitry” before reaching the light-sensitive cells so it can assumed as a back illuminated system. The "backwards" organization of rods and cones has the benefits that the retinal pigmented epithelium (RPE) can absorb scattered light. This means that vision

becomes clearer. Light can also have damaging effects, so this set up also protects the rods and cones from unnecessary damage.

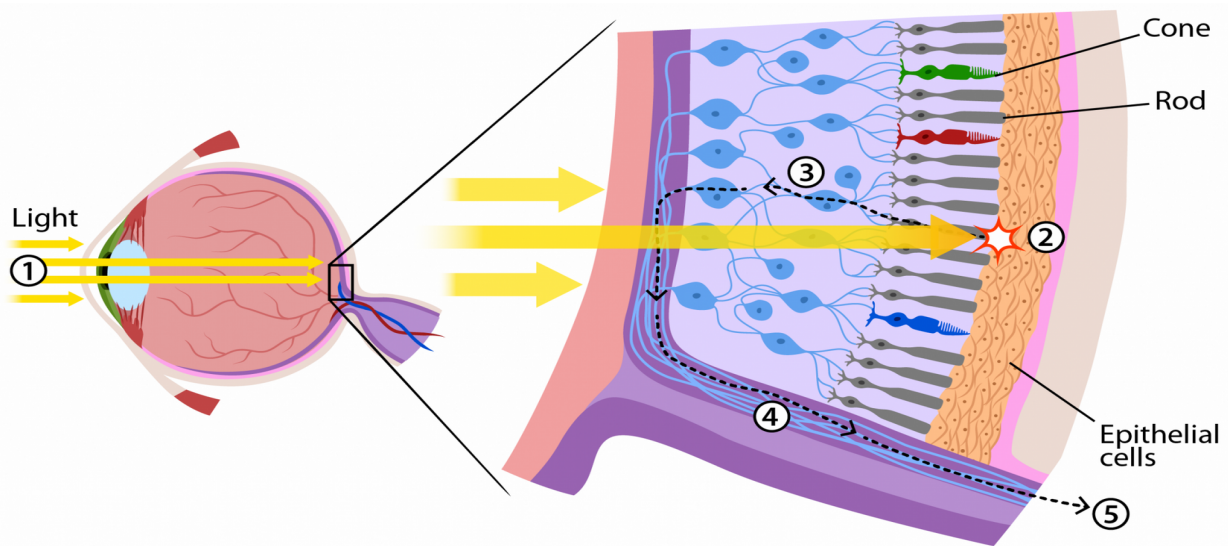


Figure 1.8: light pathway through eye

1.4.1 Rod cells

The human eye has over 100 million rod cells in the retina, providing visual capability at low light levels. They are located away from the center of retina called macula so they are responsible for peripheral or “where is it” vision. Almost 600 rods are connected to each nerve fiber in the outer part of retina thus, they are typically associated with night vision. They work so well in dim light situation because a great number of them tend to converge to a single ganglion. These ganglion cells will activate if only a certain threshold of light energy overcomes. By converging light energies from many rods to one ganglion the activation needs less effort. That’s the reason why they operate better in low light intensity.

1.4.2 Cone cells

Cone cells perform best at normal light levels, providing daytime visual facilities, including the ability to see colorful. There are roughly 6 million cone cells in the retina and they are concentrated towards the center of macula named fovea centralis. This area is responsible for detailed or “what is it” vision. The eye has 200 degrees field of view but for high resolution images the object should fall on fovea region, reducing the detailed angle at 15 degrees. The number of rods and cones are much greater than the optic nerve fibers so the connection between them is various. In the fovea there are almost one-to-one connection between cones-fibers. As the color sensitive cells cones are divided into “green” cones on a percentage of 64%, “red” cones 32% and “blue” cones about 2% based on measured response curves.

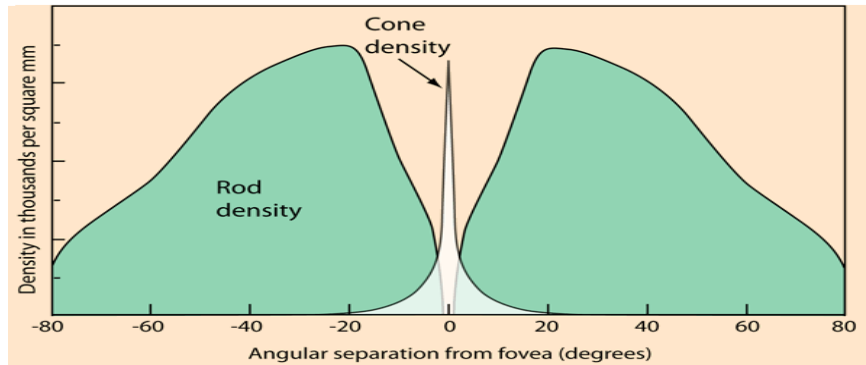


Figure 1.9: rods and cones density

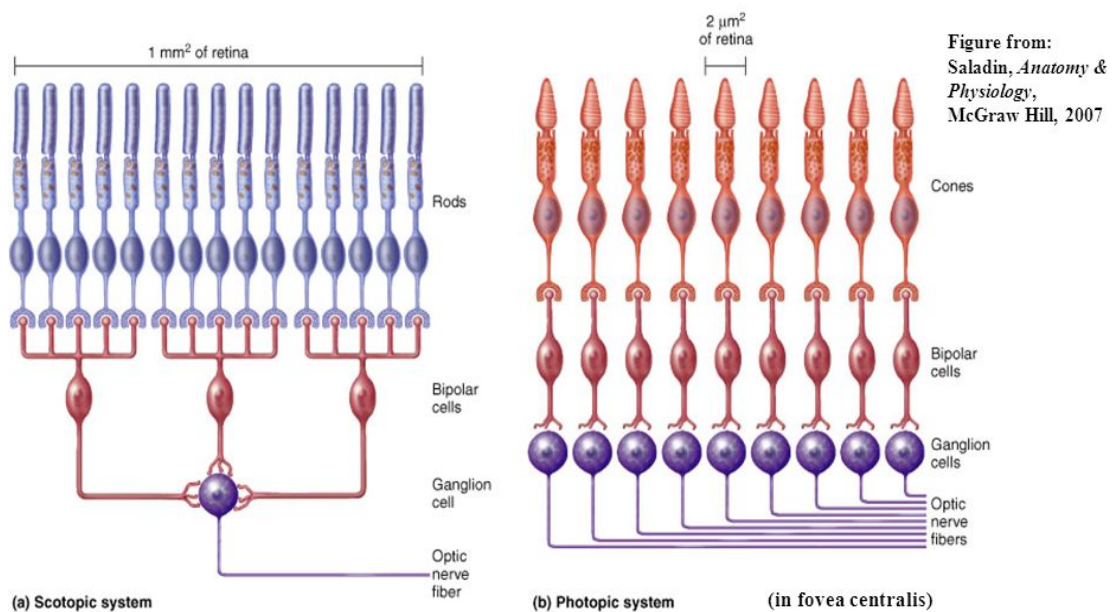


Figure 1.10: Difference in the level of convergence between rods and cones

1.4.3 Vision regimes

There are 3 different distinguishing vision regimes:

- i) Photopic Vision under well-lit conditions, which provides for color perception and functions primarily due to cone cells in the eye.
- ii) Scotopic vision which is monochromatic in very low light and functions primarily due to rod cells in the eye.
- iii) Mesopic Vision: a combination of photopic and scotopic vision in low lighting, which functions due to a combination of rod and cone cells in the eye.

Depending on the knowledge about cone and rod receptors we come to the conclusion that the relevant receptors of each vision regime are different. The figure bellow explains the relevant use of them accordingly to light levels.

ESP

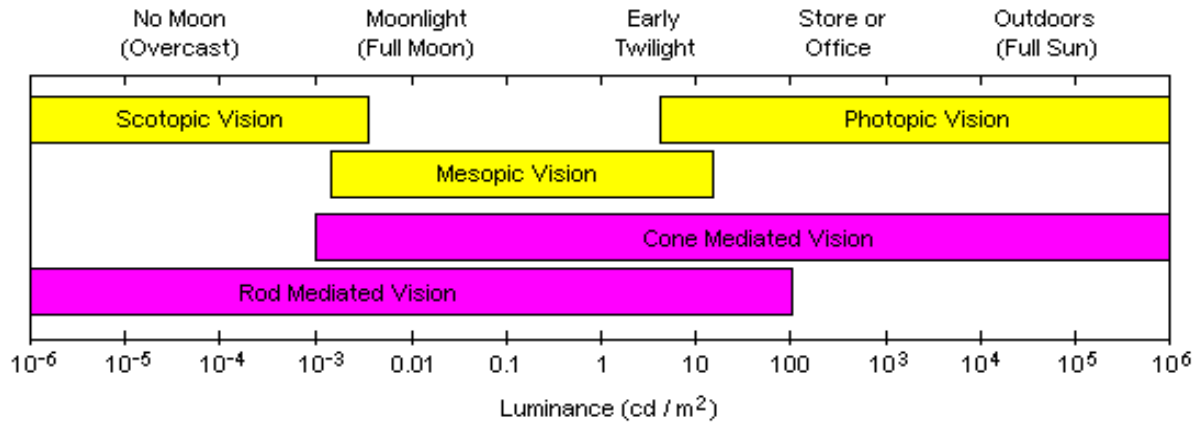


Figure 1.11: relevant receptors to each of the regimes

Chapter 2: Pupillography till today

2.1 Introduction

Understanding the clinical significance of pupil light reflex is very useful as a diagnostic tool. It allows for testing the integrity of the sensory and motor functions of the eye.[1] Pupillography can be primarily linked to the detection of abnormalities in the pupil's photomotor reflex, which however is dependent on the neurophysiology of human body and therefore is also affected by a wide variety of neurological injuries. Manual pupillary assessment can lead to significant inaccuracies and inconsistencies. Studies have shown that manual evaluation of pupillary showed low inter-examiner reliability even under identical conditions with a disagreement to be as high as 39 percent. [2][3]

2.2 Applications on diseases

Although pupillography remains underestimated. The contraction and dilation of pupil diameter is not only associated with changes in light intensity. Different neuroanatomical pathways are involved in pupil control and their neurological integrity and functionality can be often ascertained through the analysis and interpretation of the pupil reaction. There are several other factors and diseases that affect pupils behavior thus are being examined further. In this chapter will be discussed all the applications and clinical surveys that consider pupillometry as a valuable diagnostic mean.

2.2.1 Eye diseases

As obviously many eye diseases may directly affect PLR. Measuring pupillary constriction allows in vivo identification and functional assessment of eyes with optic neuritis, that will be useful in evaluating potential therapies over time. [4] An other study tried to evaluate pupillary response to light stimulation on a group of 44 patients with different stages of glaucoma using computerized pupillometry. [5] When certain circumstances are met PLR seems to be useful as additional diagnosis to indicate the occasions of cataract issues. [6]

2.2.2 Pupillography in psychology

An experiment from Hess and Polt (1960) [7] showed that pupils react not only to the changes of intensity of light but also reflect arousal or emotions. In this examination they presented specific photographs of babies and semi-naked adults. Pupils of examined people dilated after seeing the pictures of opposite sex whereas in females the dilation occurred also after seeing pictures of babies or mothers with babies. Furthermore an interesting study from Hess, Seltzer and Shlien [8] in 1965 examined pupillary responses in homosexual males, showed a greater pupil dilation to pictures of the same sex in contrast to the heterosexual. According to T.M. Simms (1967), [9] pupillary responses of males and females were greater when they were exposed to pictures of the opposite sex. Last but not least infants showed greater pupil dilation after seeing pictures of their mother than pictures of a stranger as long as when they saw pictures of faces than geometric shapes.[10]

2.2.3 Drugs and Pharmaceuticals

The effect of drugs and pharmaceuticals on the nervous system can change the pupil reflexes. In PLR any mental or emotional arousal will be combined with a pupillary reflex and could indicate the condition of a subject. Consumption of substances that affect the physiological process of nervous system could be detected through PLR. Generally it has to be concerned a lot before using such a type of examination but it may also be very useful. For example in cases of rehabilitation could be distinguished whether the will of person is strong and honest or not. The understanding of how does someone react to the idea of any substance in terms of his excitation like smell is very important. Moreover findings from previous research underscore the effect of a smoked kief preparation (*Cannabis sativa* L.) on pupil diameter variations. [11] Finally a systematic review of the correlation between antidepressants and pupil reflex reveals interesting results in the field of psychopathic medicine. Pupil dilation can be observed after either parasympatholytic or sympathomimetic drugs, and pupil constriction after parasympathomimetics or sympatholytics. The dilation speed best reflects the action of the sympathetic system while the latency of the pupillary light reflex is predominantly regulated by the parasympathetic system. By blocking the dilator muscle with dapiprazole eye drops, one can determine whether pupil dilation is caused by central inhibition of cholinergic activity. [12]

2.2.4 Diabetes and Cardiovascular Neuropathy

Diabetic autonomic neuropathy (DAN) involves most organs and diagnosis is largely based on cardiovascular tests. It is important to mention that in (DAN) pupillary autonomic dysfunction occurs before cardiovascular autonomic changes and detection of pupil denervation hypersensitivity through PLR is an inexpensive way to detect early DAN [13] In addition PLR has been used in patients with heart failure to recognize simple clinical markers that could accurately predict adverse events, especially death and hospitalization. [14] [15] It should be also noted that research has been used combining measurements from PLR and cardiovascular reflex evoked by motion pictures, to evaluate the effects of images and to avoid side effects. [16]

2.2.5 Brain and mental disorders

There are many brain or mental disorders that appear in many diseases such as Alzheimer's, Parkinson's, autism or schizophrenia. Studies have proposed that the pupillary reaction to light is deviant in schizophrenic patients compared to normal subjects. [17] In Parkinson's and Alzheimer's Disease many pupillometric variables are taken into account to evaluate them by non-invasive methods. [18] [19] An other contribution of pupillography is investigation of Myasthenia Gravis on CNS. The post-synaptic cholinergic receptor deficit may be central, within the CNS, or peripheral, related to the Neuromuscular Junction of the iris' sphincter. [20] In the autism disorder, various brain structures are involved in a way that has not been sufficiently elucidated. In surveys that have been done on children with autism spectrum disorders (ASDs), by looking at their pupillary reaction they managed to achieve up to 90 percent accuracy in their separation from those who are not autistic. It came out that participants with ASDs showed significantly longer PLR latency, smaller constriction amplitude and lower constriction velocity. [21]

2.2.6 Psychiatric disorders and anxiety

Pupillography can be a very useful tool in psychiatric disorders and anxiety behaviors. Psychosensory pupillary response is called the process where emotions such as fear, anger or stress are associated with the dilation of the pupil. Such reactions can often be confused with normal, spontaneous oscillations of pupil size, which are of the same magnitude. [22] Another research has shown that pain response may be evaluated taking advantage of the pupillography principles that are affected by factors

such as gender and anxiety. [23] Nowadays, anxiety is a common psychological issue and pupillometry is an alternative diagnostic method.

2.2.7 Alternative Cures

Beyond the limits of classical medicine, many studies are focused on traditional or alternative therapies. Surveys on the effect of acupuncture, which has a wide treating field, noticed changes in pupil's reaction when stimulating very specific points on human body. [24] Chronic headaches are studied through Kampo, the Japanese study and adaptation of the traditional Chinese medicine. This type of disease has as an effect the autonomous nervous imbalance and thus, pupil reflexes study is a window for this. A cure by a traditional medicine called “goshuyuto” remedies the balance and this is obvious through PLR [25]

2.3 Pupillometry devices

The benefits of pupillometry and its applications has triggered interest in the development of digital pupil measurement devices. This has led both researchers and companies to advance such type of devices oriented in this direction of exploiting these properties. Some examples are listed below.

VIP-300 pupillometer from NeurOptics Company. It's a monocular, hand-held device utilized for laser eye surgeries and premium Intraocular Lenses (IOLs) patients. Provides variable setting measures at scotopic, low mesopic, and high mesopic pupil sizes to stimulate daily life conditions. There is a possibility to store the data on the device or print, while the video measurement could be played on the device's screen.



Figure 2.1: VIP-300 pupillometer

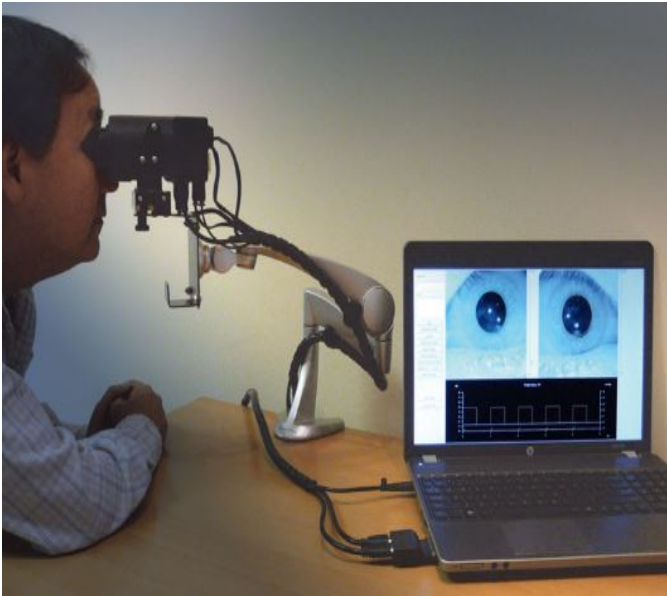


Figure 2.2: DP- 2000 Binocular Pupillometer

DP- 2000 Binocular Pupillometer, also from NeurOptics. It's a PC-based desktop system with dual cameras that measures both eyes at once providing 9 different levels of stimulating the direct, consensual, or both eyes simultaneously. Among the features are the multi-chromatic stimulation of 4 ultra bright colors, 30Hz video stream, automatic tracking and pupil detection, exports different pupil variables such as latency, diameter, constriction and dilation velocity and recovery time.

RAPD_x, from Konan Medical utilizes a high-definition, machine-vision system under controlled infrared conditions to present monocular visual stimuli while recording binocular pupil responses. The device images both direct and consensual light responses and average them into a consolidated response curve filtering the inherent noise of biological responses. In addition it allows minimally trained technical staff to collect PLR data like Resting pupil diameter, Latency, Velocity of constriction, Amplitude of constriction, Velocity of recovery.



Figure 2.3: RAPD_x pupillometer

Except the commercial, medical devices there are many research projects that raised interest in pupillography techniques. At this point will be mentioned the experimental devices developed in the optoelectronics laboratory of Technical University of Crete.

Multi-Wavelength Dynamic Imaging of the Pupillary Photomotor Reflex

A prototype model developed at the laboratory was consisted of a microcontroller for time, frequency and intensity synchronization, IR LEDs for illumination, white LEDs for stimulation, optical filters, CCD camera and an electrical supply. The arrangement of instrumentation is consecutively as shown below.

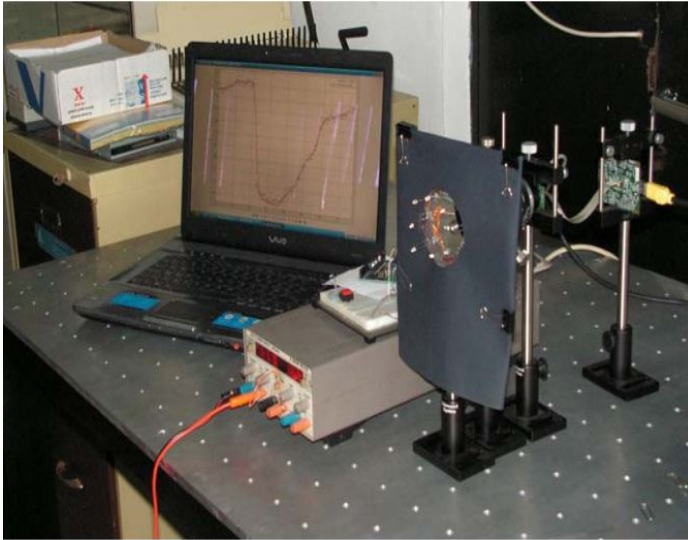


Figure 2.4 (a): *Prototype experimental model*



Figure 2.4 (b): *Prototype experimental model*

Further work on the system led to the construction of a mask that included the above elements and additionally had multi-color stimulation LEDs. This experimental device used a ski mask and has the following form.



Figure 2.5 (a): *experimental developed mask*



Figure 2.5 (b): *experimental developed mask*

Despite its functionality there there are many improvements that can be made arise from malfunctions of the old device. Among these is the non-ergonomic design because the volume and weight of the device is large enough. Likewise, the shielding

of the mask is not satisfactory, resulting in ambient light entering the area of the eye. In addition, the received images when recording the pupil contain reflection from IR LEDs and appear as white spots, making difficult the correct pupil localization and diameter estimation. Last but not least this device is wired so the remotely operation is not allowed. Although the work on this device set the basis for developing a new mask overcoming the issues of the previous one.

2.4 Statement of purpose

Traditionally, pupil measurements have been performed in a very subjective manner by using a penlight or flashlight to manually evaluate pupil reactivity and using a pupil gauge to subjectively estimate pupil size. Therefore the probability of error increases significantly. The same study that testify the inter-examiner disagreement concluded that automated pupillometry is a necessary tool for accuracy and consistency in pupil measurement and that it might allow earlier detection of subtle pupil changes, providing more effective and timely diagnostic and treatment interventions. [2]

Automated, computerized pupillometry is reliable, objective measurement of pupillary size and eliminates subjectivity. Offers the possibility of exporting accurate and trendable pupil data on a fast, painless and non-invasive process. It's independent of examiner, resulting in a significant quality improvement for various examination.

Chapter 3: Device instrumentation

Depending on previous work accomplished in Optoelectronics Laboratory, searching about the new technologies and analyzing the requirements of our new system, we reached to develop a wireless mask utilizing:

- a virtual reality mask (VR)
- two raspberry Pi Zero Wifi
- two raspberry cameras
- two TLC5940 microcontrollers
- arduino nano
- 8 infrared LEDs for illumination
- 24 LEDs and their resistors for stimulation
- batteries, battery charger, boost converter and a switch
- 2 light diffusers

The arrangement between these elements is presented in a block diagram:

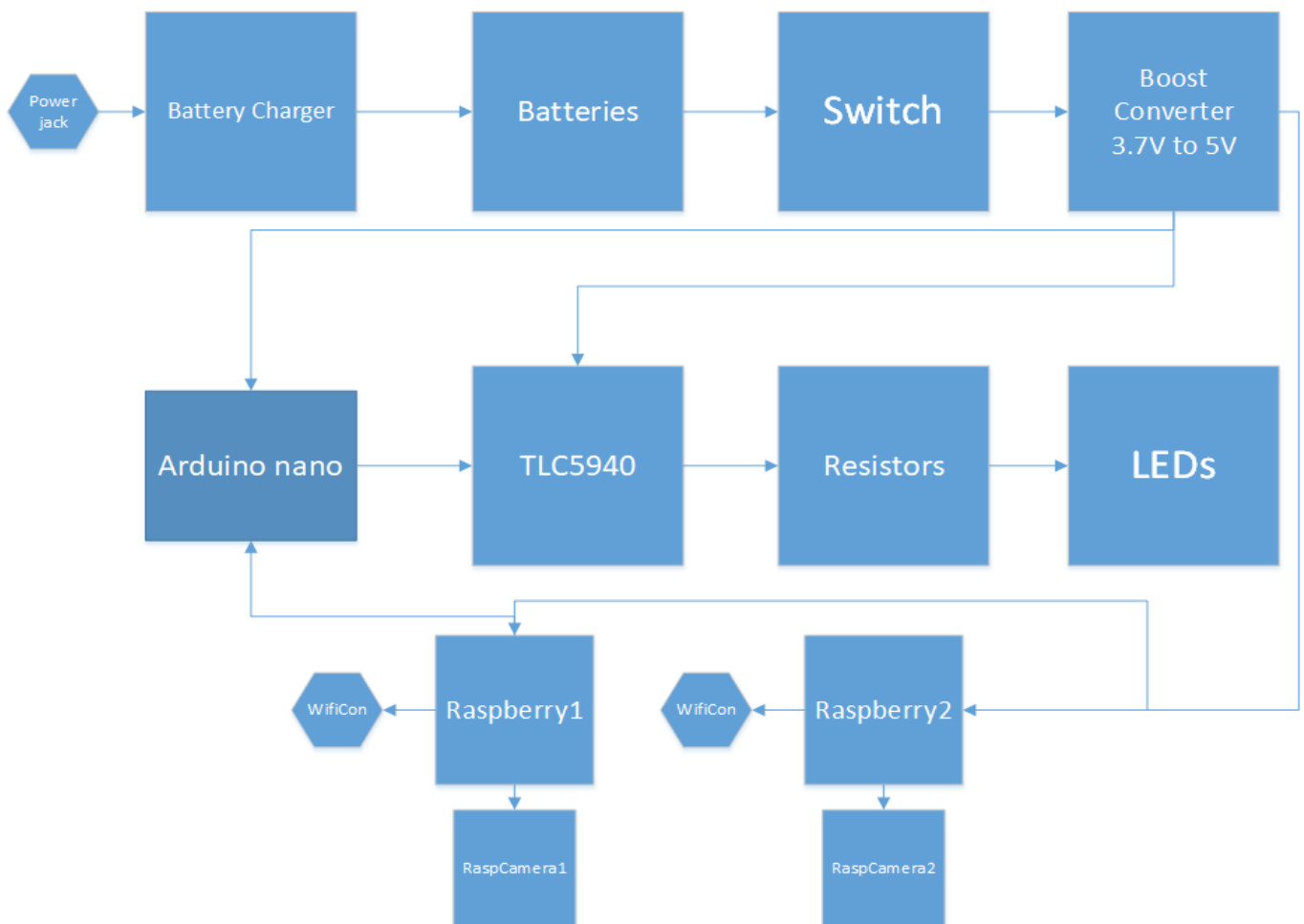


Figure 3.1: Schematic block diagram of all components

3.1 virtual reality mask

Reaching the ending of 2017, virtual reality established in many lives. VR masks became very popular such as the applications like games, movies, educational or medical projects, etc. Based on the same logic the device that chosen is BlitzWolf® BW-VR3 3D VR Glasses Virtual Reality Headset



Figure 3.2: VR mask

Technical characteristics:

Compatible Screen Size 3.5" to 6.3"
Maximum Smartphone Size Length: 168mm; width: 83.5mm; depth:13mm
Lens 2 * 42mm Mitsubishi PMMA Aspherical Lenses (FOV108°)
Pupil Distance Adjustment 55mm-65mm
Focal Distance Adjustment 56-60mm
Material ABS shell & soft artificial perforated leather straps
Weight 390g(glasses)+150g(package)
VR3 Dimensions 200*107*140mm
Color Black

3.2 raspberry Pi Zero Wifi

A small dimension, open source platform preferred depending on the requirements. Additionally it provides wireless communication, one of the main advantages of the advanced system. Moreover the architecture was based on use of raspberry cameras providing sufficient features for the demands of the application.

Technical characteristics:

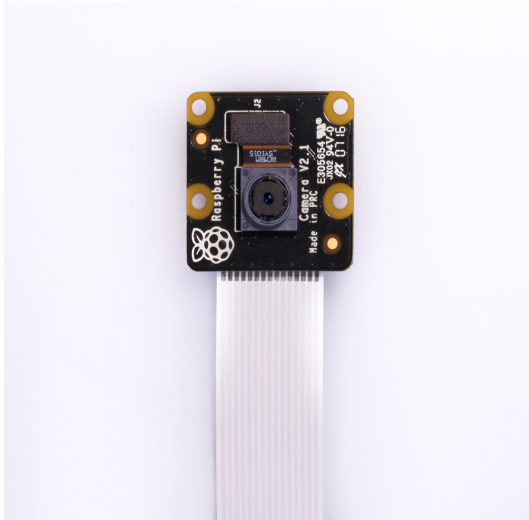
Dimensions: 65mm × 30mm × 5mm
CPU: ARM11 running at 1GHz
RAM: 512MB
Wireless: 2.4GHz 802.11n wireless LAN
Bluetooth: Bluetooth Classic 4.1 and Bluetooth LE
Power: 5V, supplied via micro USB connector
Video & Audio: 1080P HD video & stereo audio via mini-HDMI connector
Storage: MicroSD card
Output: Micro USB
GPIO: 40-pin GPIO, unpopulated
Pins: Run mode, RCA composite Camera Serial Interface (CSI)



Figure 3.3: raspberry Pi Zero Wifi

3.3 raspberry camera module

The v2 Pi NoIR has a Sony IMX219 8-megapixel sensor. This camera module does not employ an infrared filter offering the ability to see in the dark with infrared lighting and a fixed focus lens. It's a leap forward in image quality, color fidelity, and low-light performance.



Technical characteristics:

Board size: 25mm x 23mm x 9mm

Weight: 3g

Lens: fixed focus lens on-board

Field of View: customizable

3280 x 2464 pixel static images

Video: 1080p30, 720p60, 640x480p60/90

No Infrared filter

Optical size of 1/4"

1.4 μm X 1.4 μm pixel

Figure 3.4: raspberry camera

3.4 arduino nano

The Arduino Nano is a small, complete, and breadboard-friendly board based on the ATmega328 8-bit AVR microcontroller. First exertion was composed of only the raspberries. However the LEDs flickering problem led the implementation to use ATmega328 microcontroller. Finally the signals from raspberry are transmitted to Arduino nano which in respect controls the necessary input signals of TLC5940 microcontroller which is presented below.

Technical characteristics:

-**Microcontroller** ATmega328

-**Operating Voltage** 5 V

-**Flash Memory** 32 KB of

-**SRAM** 2 KB

-**Clock Speed** 16 MHz

-**Input Voltage** 7-12 V

-**PWM Output** 6

-**Power Consumption** 19 mA

-**PCB Size** 18 x 45 mm

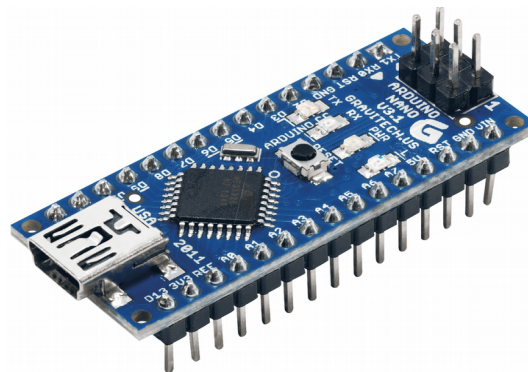


Figure 3.5: arduino nano

3.5 TLC5940 microcontroller

TLC5940 from Texas Instruments, is a 16-channel Led Driver. Each channel has an individually adjustable 4096-step grayscale pulse width modulation (PWM) brightness control and a 64-step, constant-current sink (dot correction). Both grayscale control and dot correction are accessible through a serial interface. The maximum current value of all 16 channels can be controlled via a single external resistor. In this implementation two TLC5940 microcontrollers are connected in series to enable more than 16 LEDs cascading the signals.



Figure 3.6: TLC5940 microcontroller

Technical characteristics:

-16 Channels

-12 bit (4096 Steps) Grayscale PWM Control

-Dot Correction 6 bit (64 Steps)

Storable in Integrated EEPROM

-Drive Capability (Constant-Current Sink)

0 mA to 60 mA ($V_{CC} < 3.6 \text{ V}$)

0 mA to 120 mA ($V_{CC} > 3.6 \text{ V}$)

-LED Power Supply Voltage up to 17 V

- $V_{CC} = 3 \text{ V}$ to 5.5 V

-Serial Data Interface

-Controlled In-Rush Current

-30 MHz Data Transfer Rate

-CMOS Level I/O

-Error Information

LOD: LED Open Detection

TEF: Thermal Error Flag

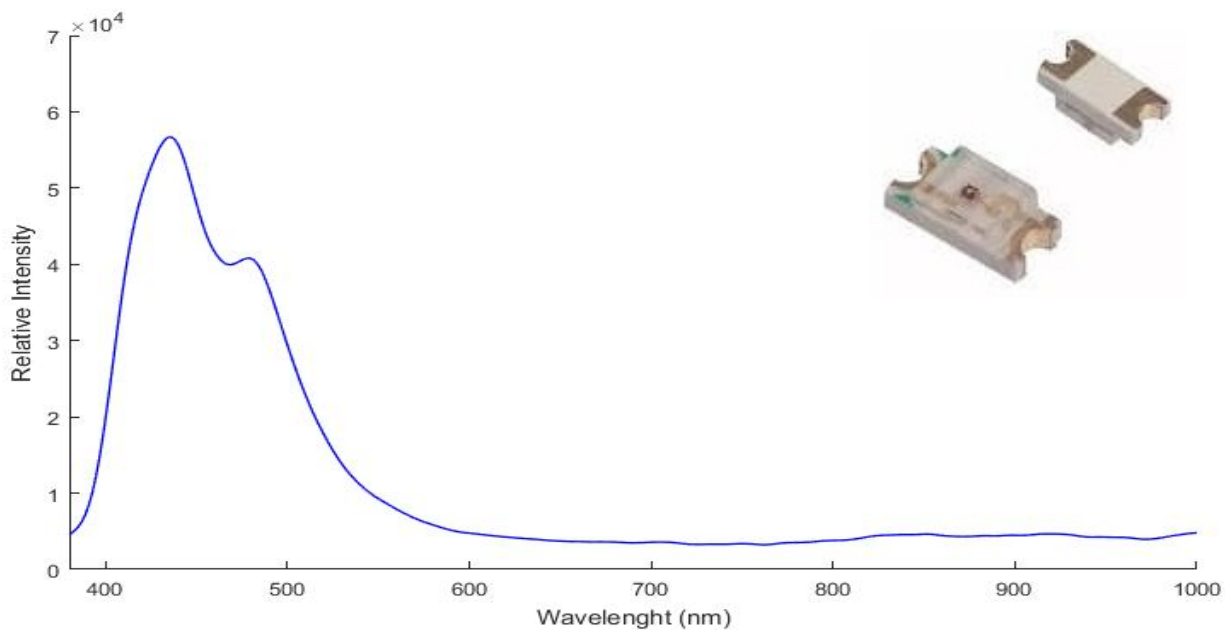
3.6 Leds and resistors

In this application LEDs are used as a light stimulation to enable the oculomotor reflex and make it possible to capture pupils' reactions. Selected LEDs are surface mount devices (SMD) and spread out almost all the visible spectrum. Different wavelengths contribute to a different pupil reaction due to varied density of cone cells, as described above. The LEDs are divided into two same groups for each eye. In each group there are two sets of 11 monochromatic LEDs interdimensionally surrounding the margin of eye, one white LED and 4 infrared (IR) LEDs. The logic behind the use of IR LEDs is the dome illumination during the procedure because the VR mask is shielded in order to prevent ambient light reach humans eye. Furthermore the pupil size will not be influenced because of IR radiation is above the visible

spectrum. As a result of different forward voltage values of every LED a need came out to control the output voltage of TLC5940 microcontrollers' outputs. In such wise resistors are used to limit down the voltage value in permissible limits. Finally, 2 light diffusers settled down, after the placement of these components and the functionality testing to provide dome light illumination without creating white spots on eye image.

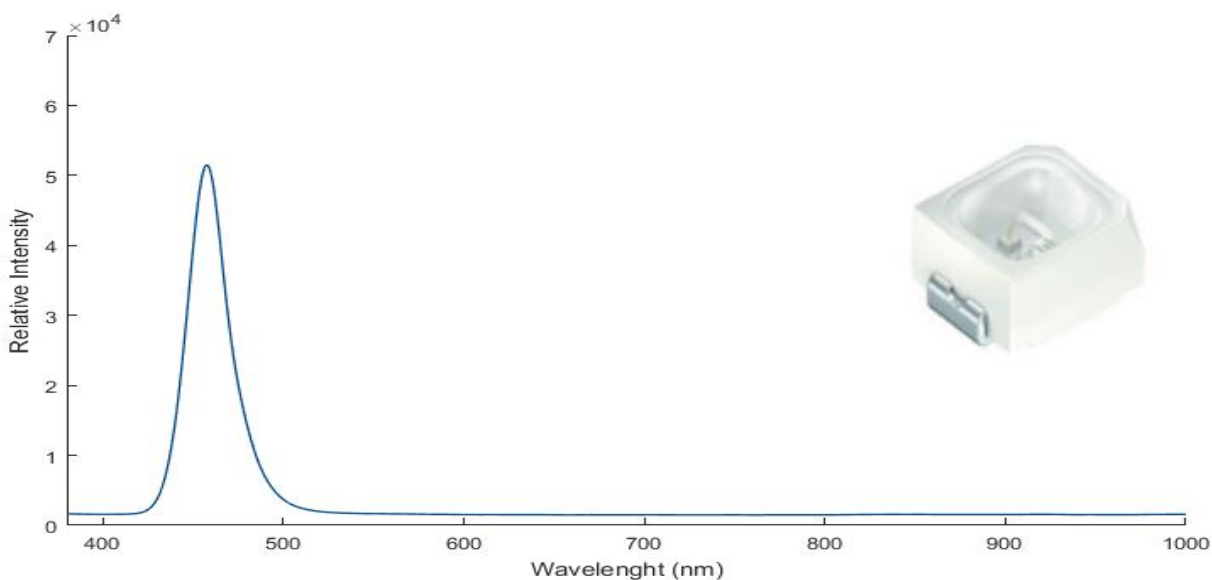
430nm led

This LED has a water clear lens and it's blue SMD LED by VCC, model CMD15-21UBC/TR8. The peak wavelength is $\lambda_{\text{peak}} = 430\text{nm}$, FOV = 140° and forward voltage $V_f = 4,9\text{ V}$.



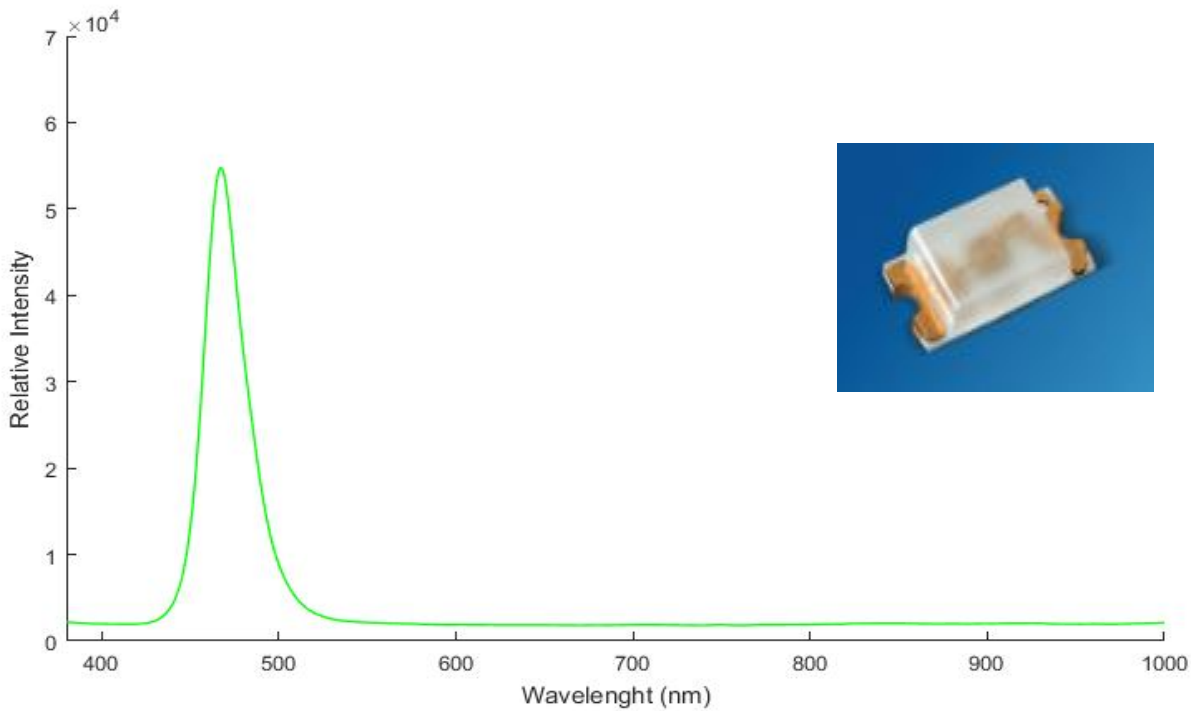
460nm led

This LED has a clear lens and it's blue SMD LED by OSRAM, model LD MVSG-JGLH-46-1. The peak wavelength is $\lambda_{\text{peak}} = 460\text{nm}$, FOV = 120° and forward voltage $V_f = 3.05\text{ V}$.



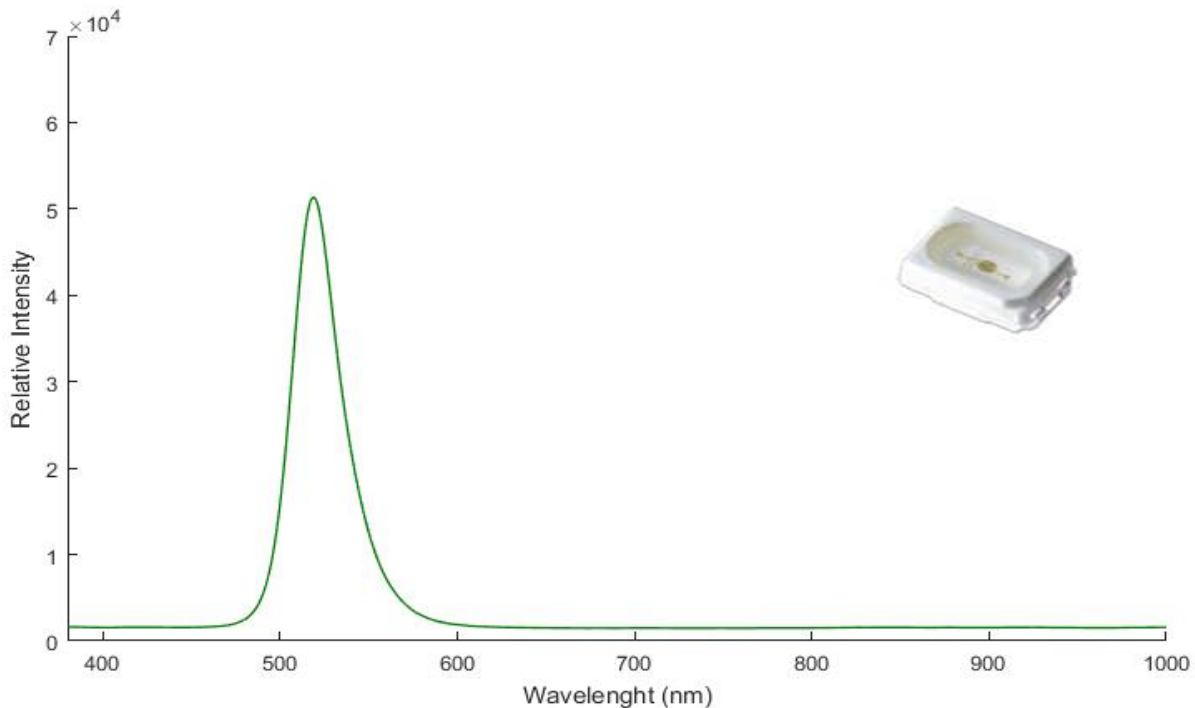
470nm led

This LED has a colorless diffused lens and it's blue SMD LED by OSRAM, model LB Q39G-L200-35-1. The peak wavelength is $\lambda_{\text{peak}} = 470\text{nm}$, FOV = 170° and forward voltage $V_f = 2.85\text{ V}$.



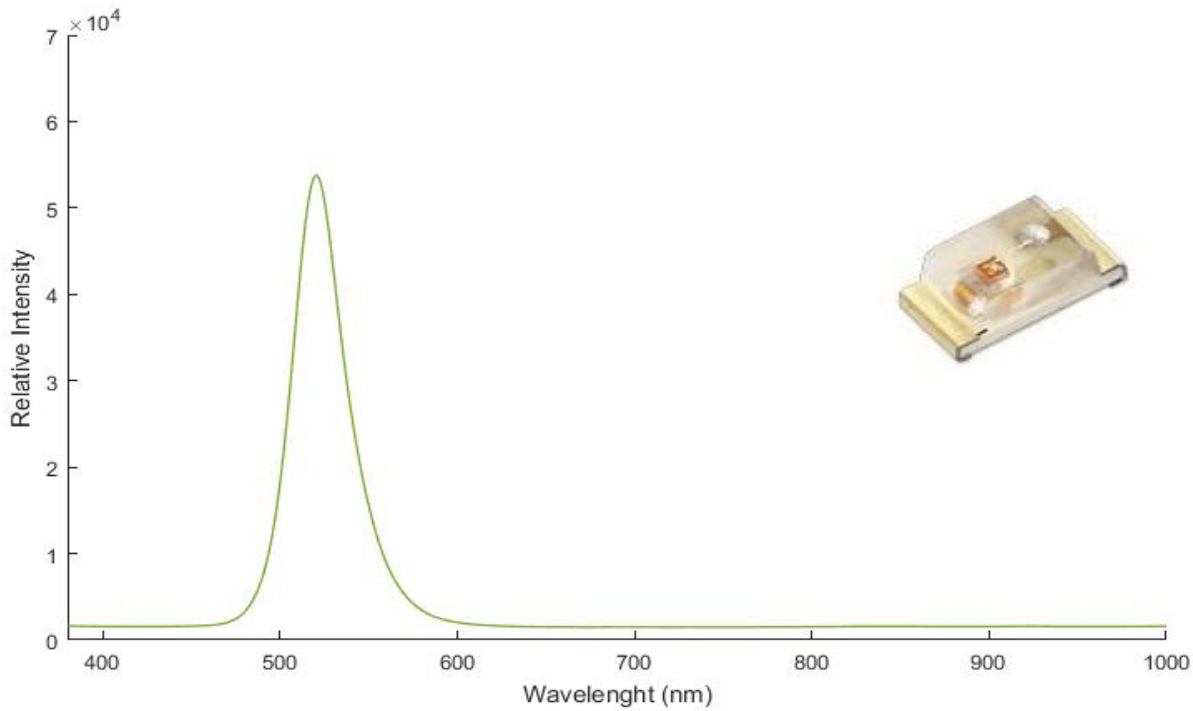
515nm led

This LED has a water clear lens and it's green SMD LED by Kingbright, model AA3021ZGSK. The peak wavelength is $\lambda_{\text{peak}} = 515\text{nm}$, FOV = 125° and forward voltage $V_f = 3.3\text{ V}$.



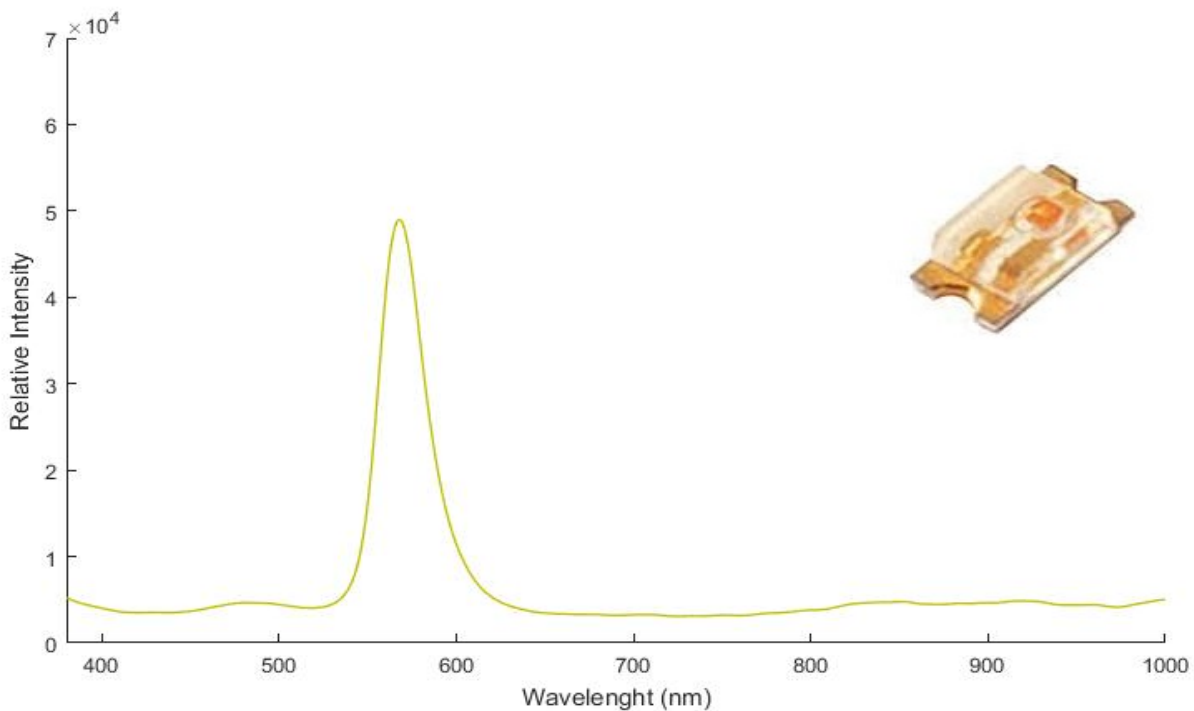
535nm led

This LED has a water clear lens and it's green SMD LED by Kingbright, model APT1608VGC/Z-PRV. The peak wavelength is $\lambda_{\text{peak}} = 535\text{nm}$, FOV = 120° and forward voltage $V_f = 3.2\text{ V}$.



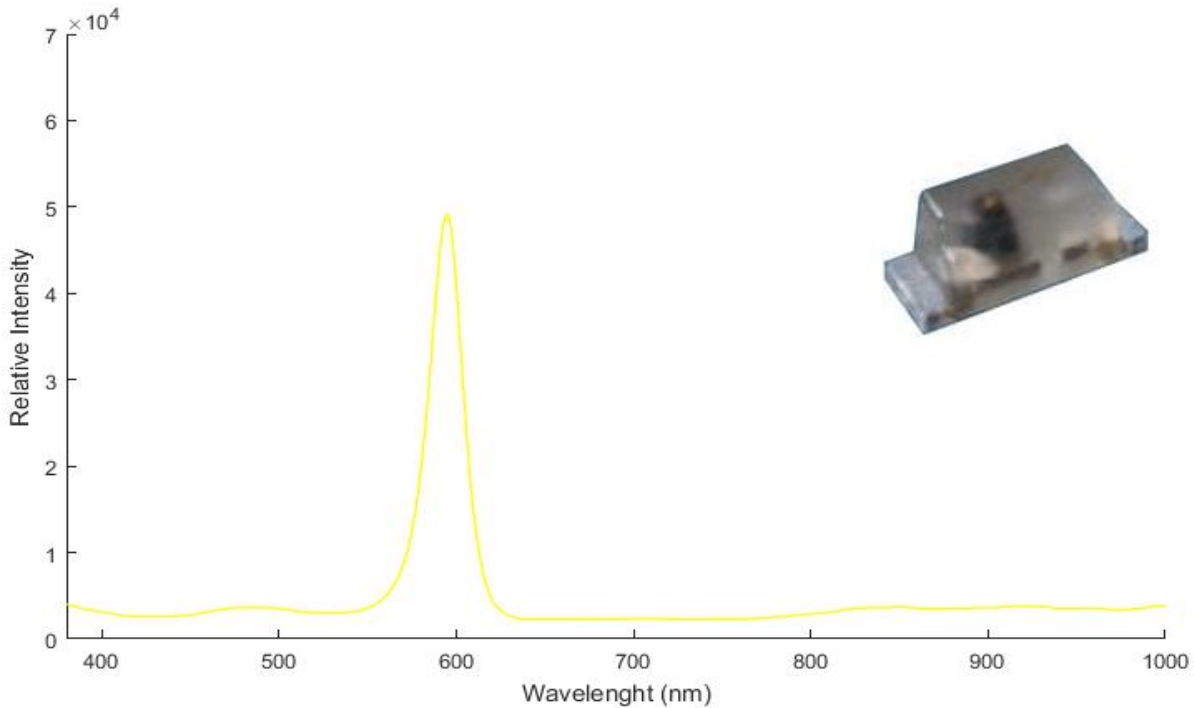
569nm led

This LED has a water clear lens and it's green SMD LED by Lite-On, model LTST-C190GKT. The peak wavelength is $\lambda_{\text{peak}} = 569\text{nm}$, FOV = 130° and forward voltage $V_f = 2.1\text{ V}$.



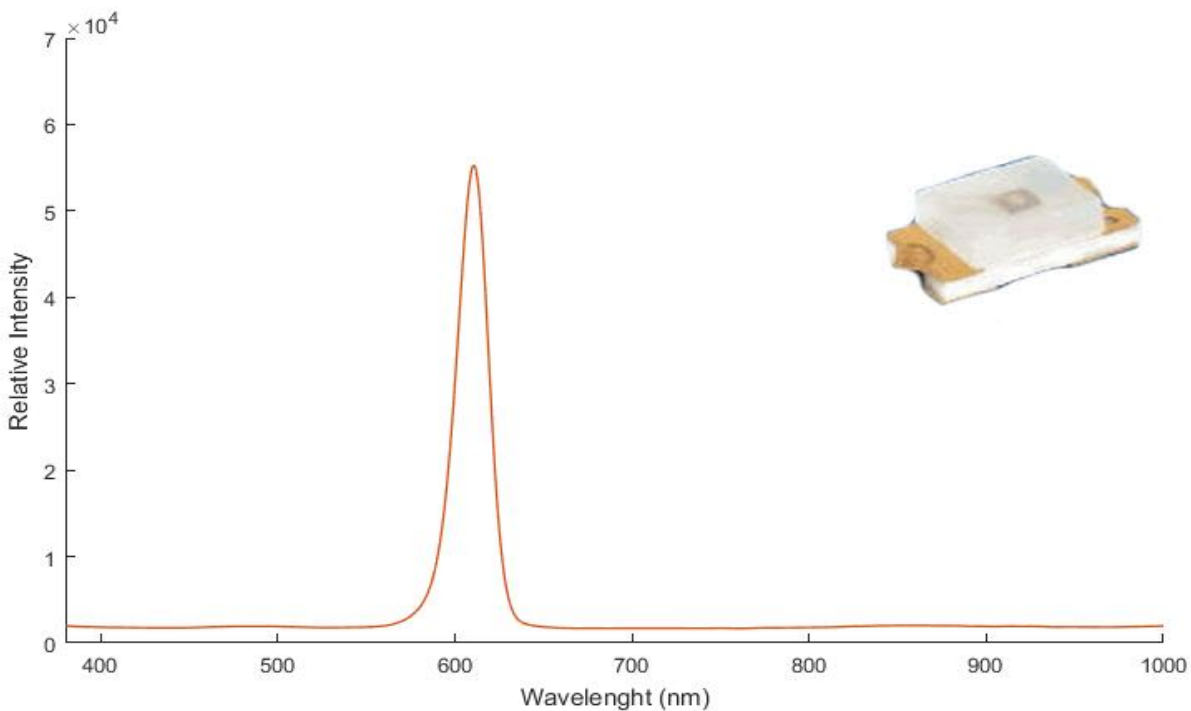
587nm led

This LED has a colorless diffused lens and it's yellow SMD LED by OSRAM, model LY L29K-H1K2-26-Z. The peak wavelength is $\lambda_{\text{peak}} = 587\text{nm}$, FOV = 160° and forward voltage $V_f = 2.2\text{ V}$.



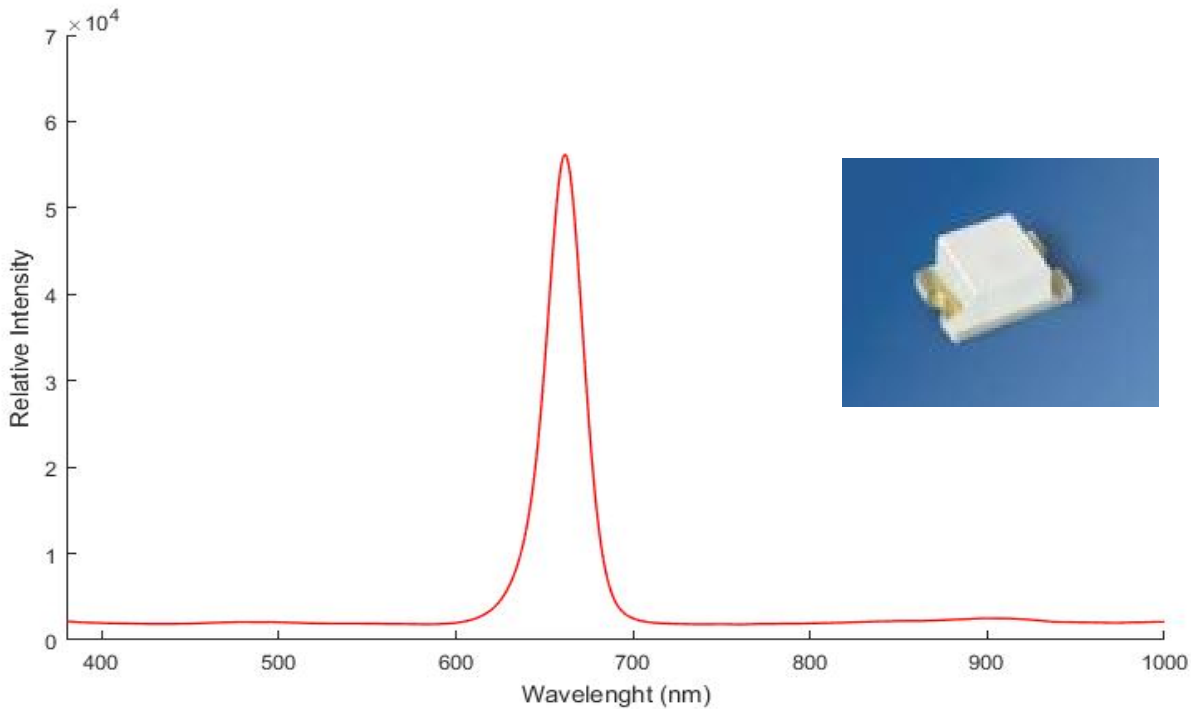
605nm led

This LED has a colorless diffused lens and it's orange SMD LED by OSRAM, model LO Q976-PS-25. The peak wavelength is $\lambda_{\text{peak}} = 605\text{nm}$, FOV = 160° and forward voltage $V_f = 2.5\text{ V}$.



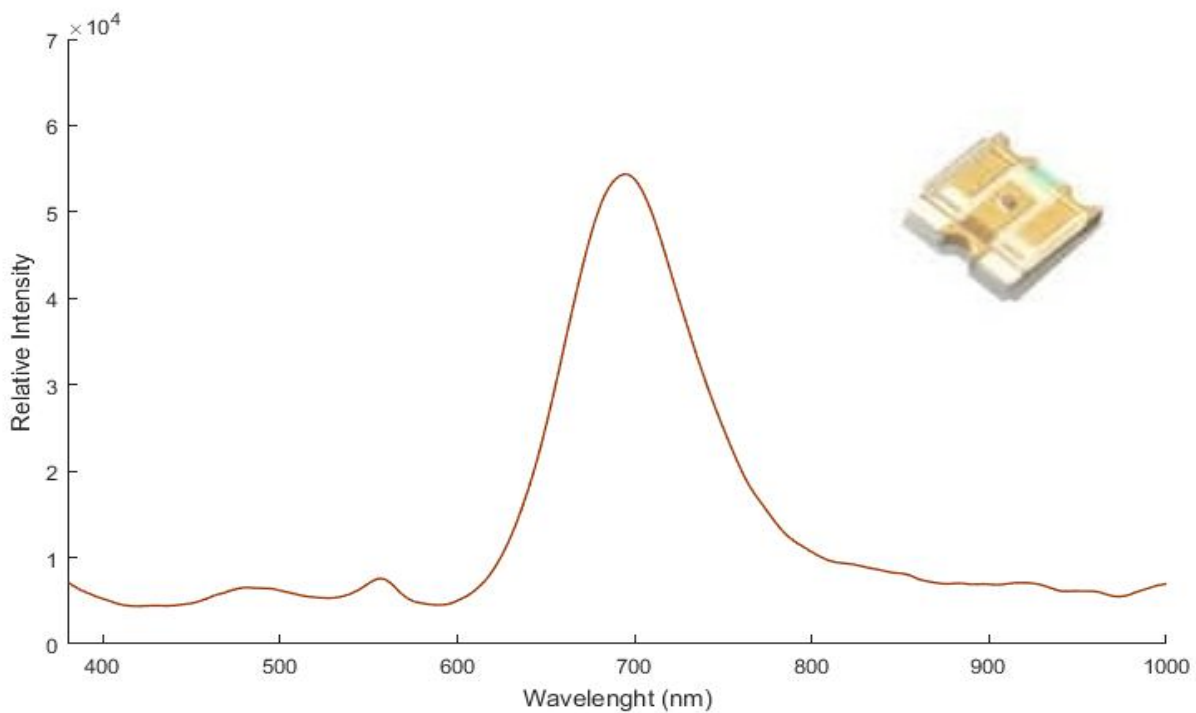
645nm led

This LED is a red SMD LED by OSRAM, model LH R974-LP-1. The peak wavelength is $\lambda_{\text{peak}} = 645\text{nm}$, FOV = 160° and forward voltage $V_f = 1.8\text{ V}$.



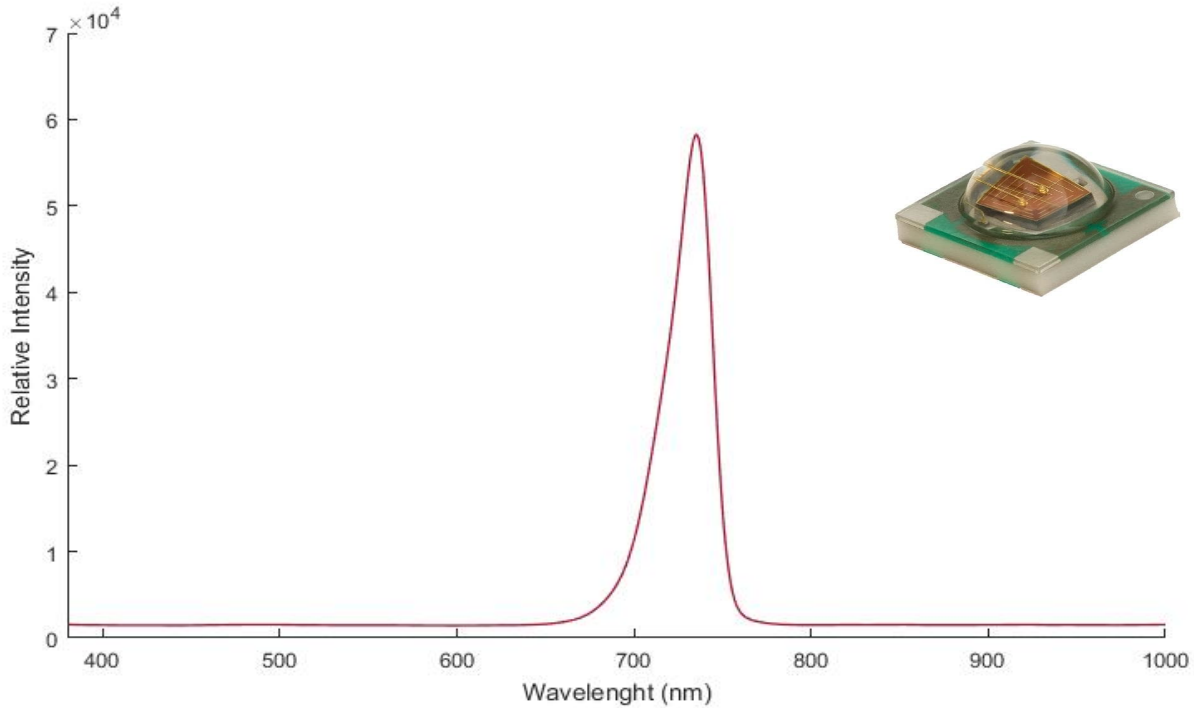
700nm led

This LED has a clear water lens and it's red SMD LED by Lumex, model SML-LX15HC-RP-TR. The peak wavelength is $\lambda_{\text{peak}} = 700\text{nm}$, FOV = 140° and forward voltage $V_f = 2\text{ V}$.



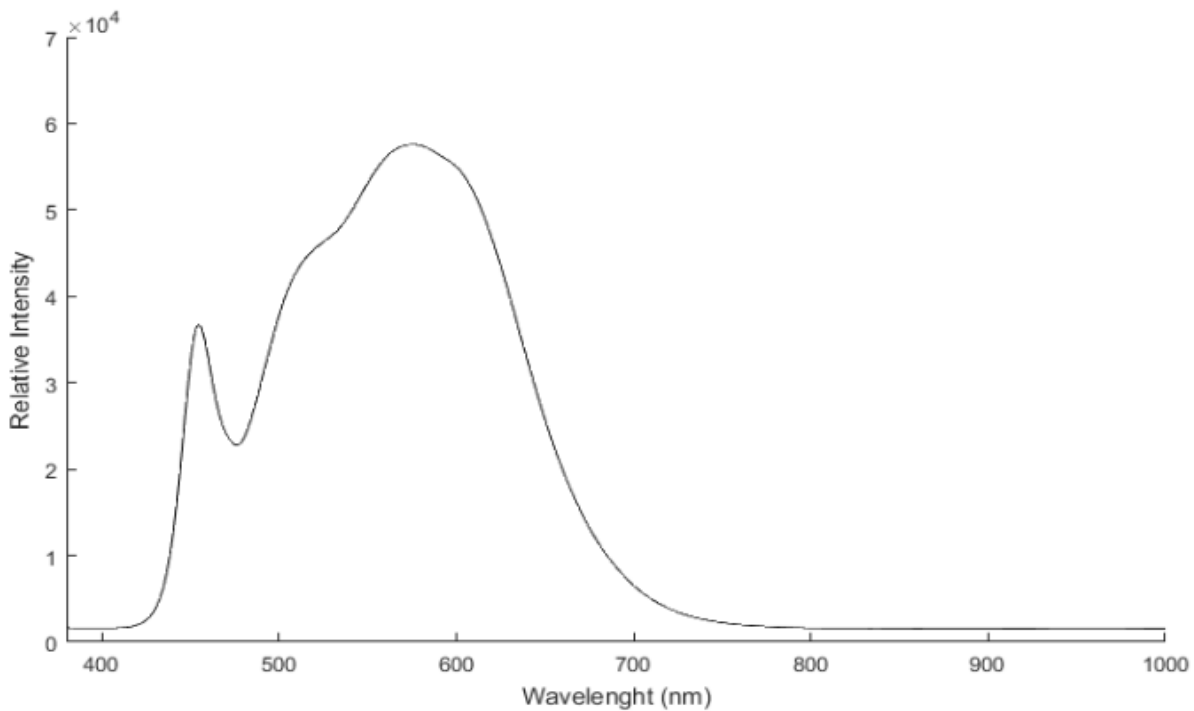
730nm led

This LED is far red SMD LED by CREE, model XPEFAR-L1-0000-00601. The peak wavelength is $\lambda_{\text{peak}} = 730\text{nm}$, FOV = $115^\circ\text{-}130^\circ$ and forward voltage $V_f = 1.9\text{ V}$.



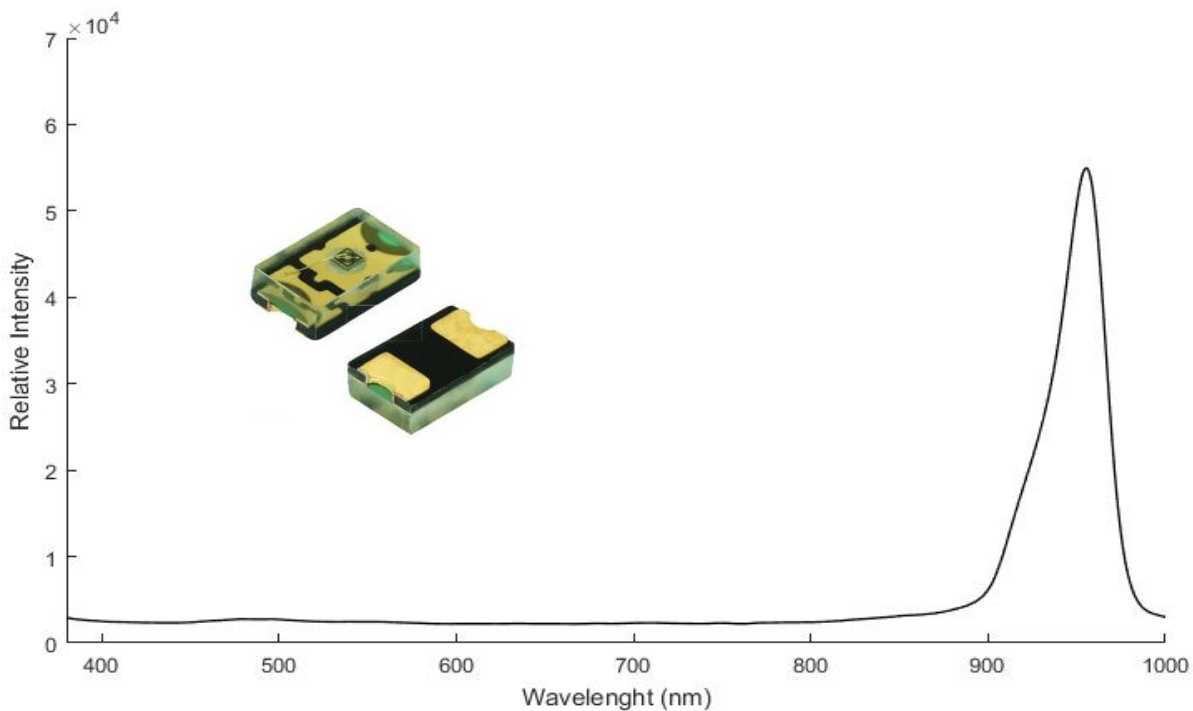
white led

This LED is warm white SMD LED by NICHIA, model NSSL157AT-H3 with FOV = $115^\circ\text{-}130^\circ$ and forward voltage $V_f = 3\text{ V}$



IR led

This LED is infrared SMD LED by Vishay, model VSMB1940X01. The peak wavelength is $\lambda_{\text{peak}} = 940\text{nm}$, FOV = 60° and forward voltage $V_f = 1.35\text{ V}$.



3.7 Batteries, charger, converter, monitor and a switch

In order to create a wireless, autonomous, embedded system batteries are significant to operate without a need of external power supply. Two batteries of 3400 mAh each was preferred offering the capability of long time operating and stored inside the VR mask. As long as the batteries are rechargeable a battery charger required as much as a boost converter to step up the voltage and satisfy the requirements of the system. Eventually a switch adjusted to turn off the power supply and a battery monitor to track the battery level.



Figure 3.7: rechargeable batteries

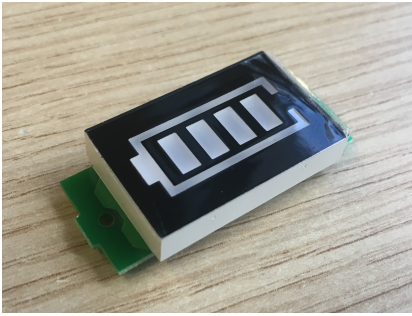


Figure 3.8: battery monitor



Figure 3.9: battery converter



Figure 3.10: battery charger

Since all material requirements had analyzed, we created the final PCB circuit and tested all the connections to avoid short circuits. Below are presented the PCB wiring diagram, the front and rear view.

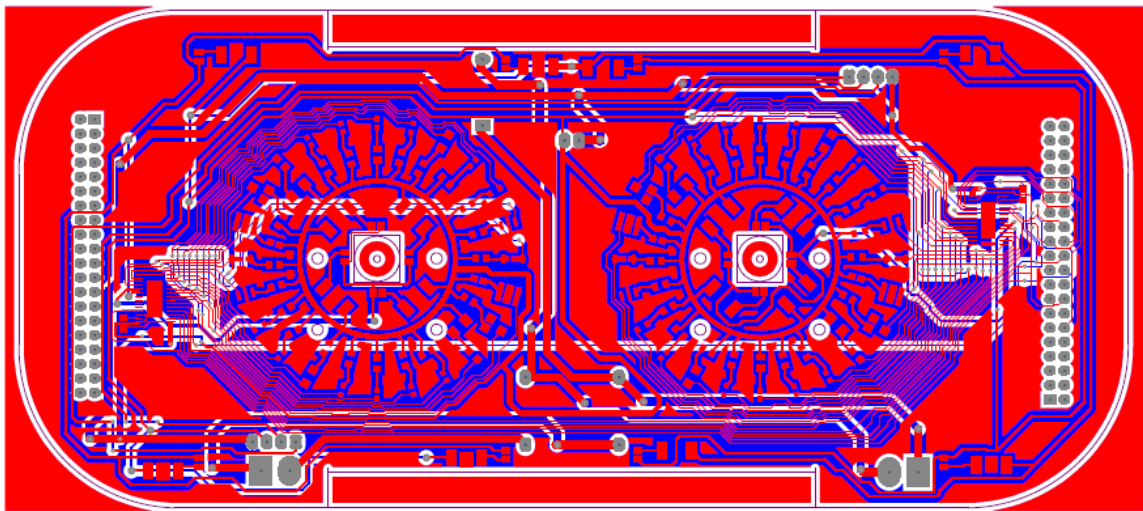


Figure 3.11: PCB wiring diagram

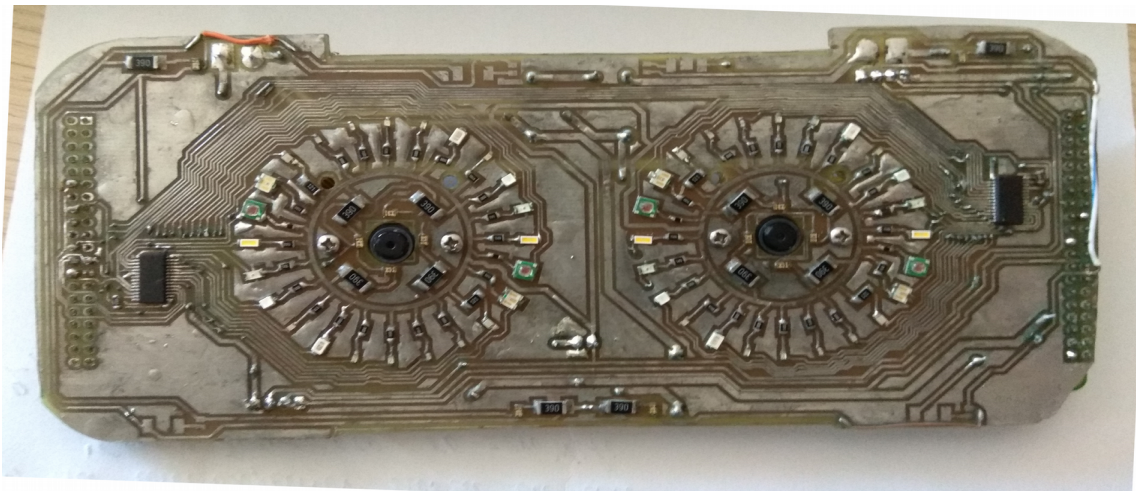


Figure 3.12: PCB front view

Multi-Wavelength Dynamic Imaging of the Pupillary Photomotor Reflex

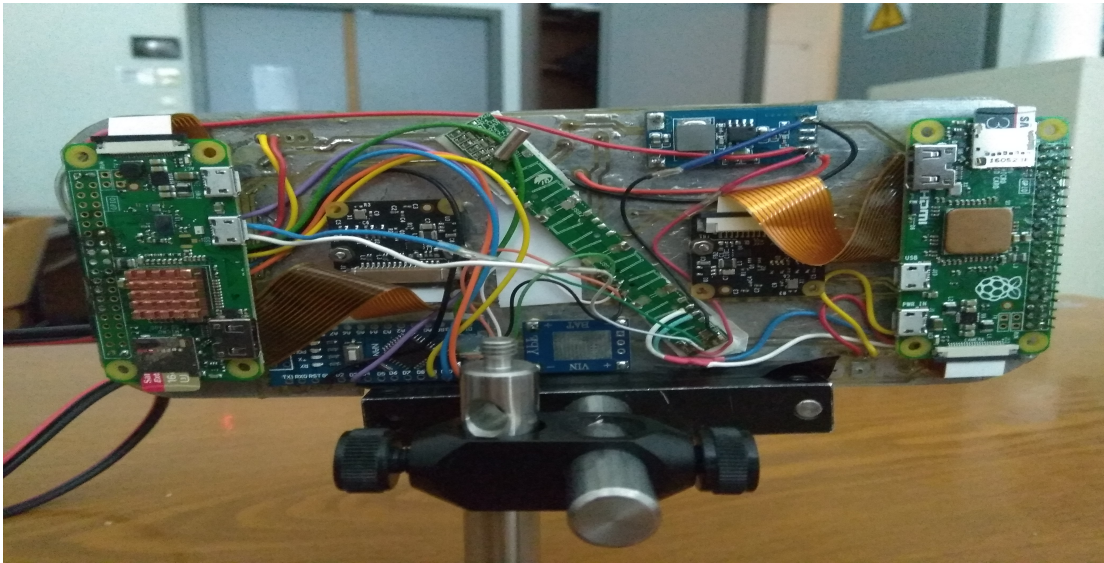


Figure 3.13: PCB rear view

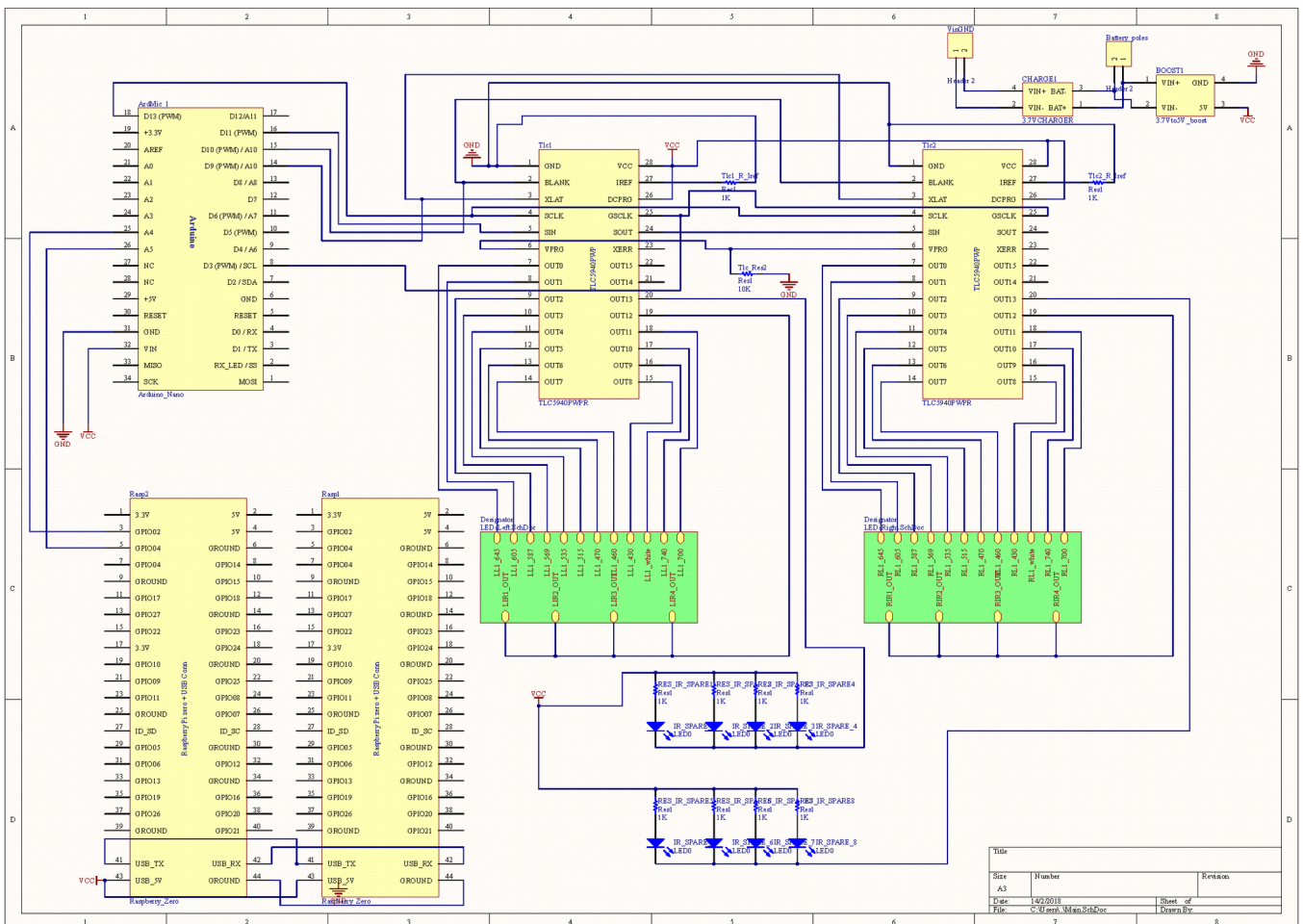


Figure 3.14: Schematic wiring diagram of all components

Chapter 4: Software Development

4.1 LEDs driving procedure

The proposed system uses visual stimuli from 24 LEDs for each eye as mentioned above. These LEDs are located at the perimeter of the camera recording the PLR and are placed in groups of two, counter-diametrically so that the examined does not stare towards the light and move his eye. This set-up contribute to avoid the possibility of capturing blurred images during the examination. Although the initial experimental setup was consisted of a breadboard, raspberry pi 3 Model B, TLC5940 microcontroller, LEDs and resistors. TLC5940 microcontroller was powered by 5V supply from raspberry pi 3 and some LEDs and resistors were connected on its output to check the functionality of led driving algorithm. For that reason a library that connects raspberry systems with TLC5940 microcontroller was used to communicate between these two components and control the output selection and the dimming value. The same algorithm was tested on the developed PCB to examine the functionality of whole system with the proper signals being eventually transferred through the ATmega328 to the TLC5940 microcontroller

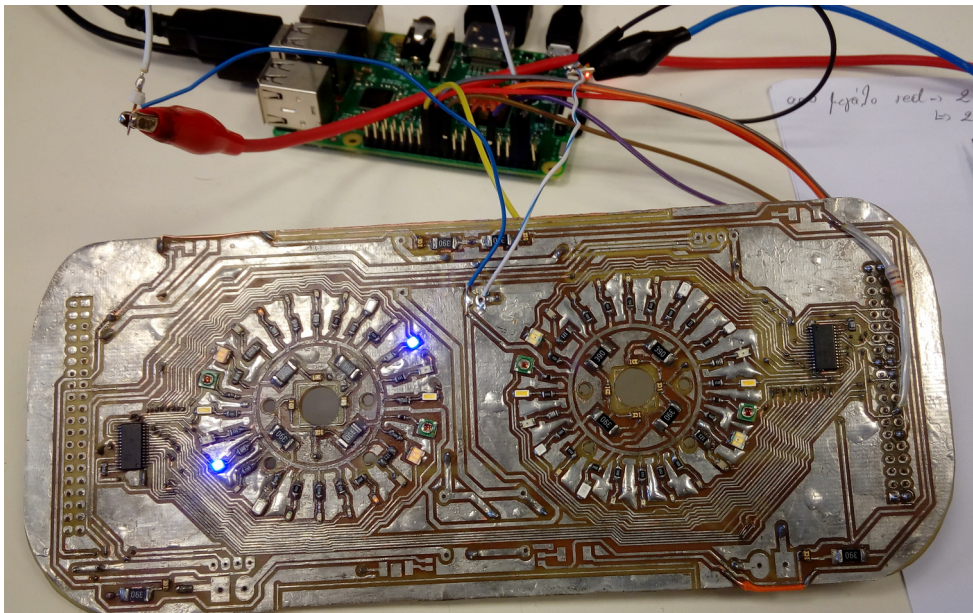


Figure 4.1: LEDs functionality control

To control the LEDs an algorithmic procedure was developed to choose a specific wavelength stimulation, duration of exposure and dimming value. The design that implements this process is shown in the figure below.

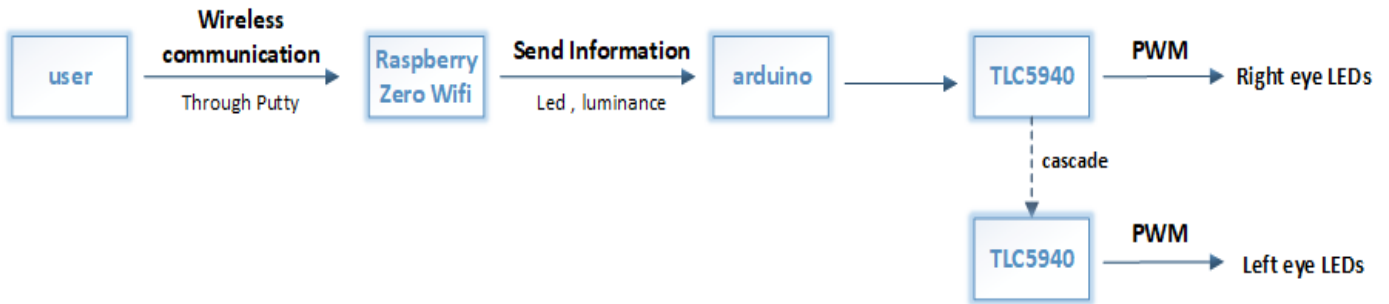


Figure 4.2: LEDs control algorithmic procedure

Starting from the user of the system, who is supposed to be the examiner, a communication must be established with the raspberry. In this case PuTTY is used as an open-source, terminal emulator for text-based communication between multi-platform applications capable of executing in most operating systems. After the establishment of communication with raspberry a camera control software is executed developed in optoelectronics laboratory. Through raspberry an algorithm written in C++ is executed to choose a LED as a stimulation and the intensity value for a given time slot. This information is transferred to ATmega328 microcontroller of arduino nano which controls the input values of TLC5940 microcontroller. To complete the action of LED driving circuit the TLC5940 sends a PWM signal to selected LED. This microcontroller has 16 PWM outputs thus a cascading of signals to a second microcontroller is needed which will be refer to the LEDs of other eye stimulation.

4.2 Qt GUI and layout

The software development was implemented in Qt environment which is a cross-platform application framework and is also used for developing graphical user interfaces (GUIs). As an extension of the camera control software that is also implemented in Qt, a new layout was created, integrating all the extensions needed to examine the PLR.

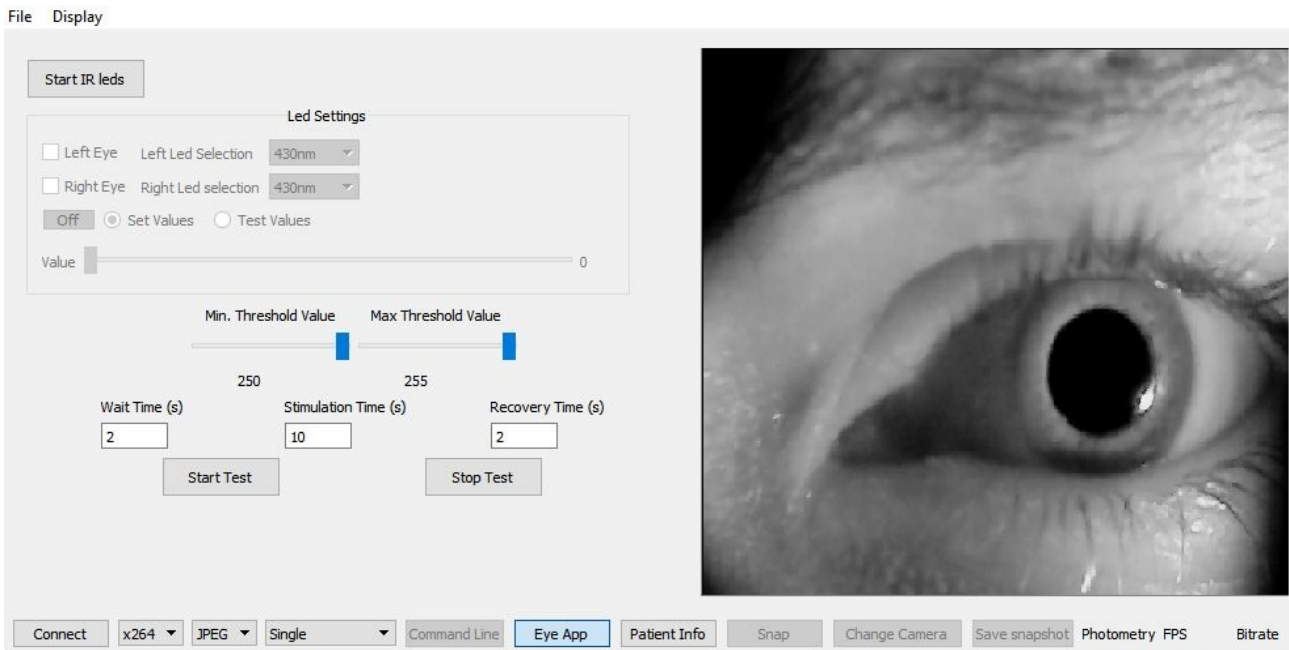


Figure 4.3: GUI layout to adjust program parameters

After having established the wireless communication with raspberry Zero, cameras start their operation to capture pupil's reaction and the video is projected on the right side of GUI. Afterwards the IR LEDs are activated to provide dome illumination without interact pupil size. At this point a set of parameters is defined for choosing right or left eye and the visual stimulation. Also there is an opportunity to select specific wavelength and illumination for the examination while three time variables must be specified to start the procedure. These variables define the time steps during the examination. When the mask is attached and everything is ready to start capturing the process will wait for a given wait time. Then the selected LED will power on for stimulation time to activate the PLR. Eventually the LED will power off and the procedure will wait for a given recovery time to restore pupil size. In the end the information of pupil diameter are stored before finishing the examination. The graphic diagram is then calculated from the results of the measurement values.



Figure 4.4: time steps

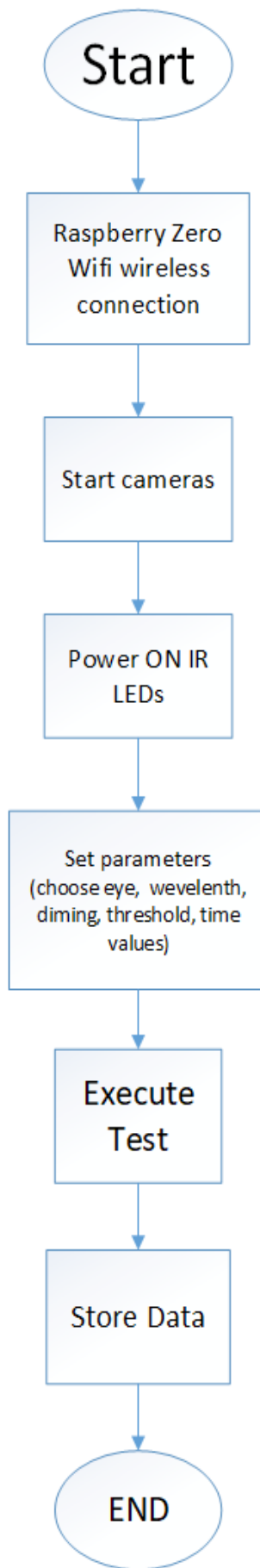


Figure 4.5: PLR test flow diagram

One more page was added as a layout that allows the patient's personal information to be imported. Once these are completed, they are stored in the same excel file with the patients measurements.

File Display

Patient Info

Last Name First Name

Date of birth: Day Month Year

City Address

Home phone Mobile Phone

Notes

Connect x264 JPEG Single Command Line Eye App Patient Info

Figure 4.6: Patient Info page

4.3 Pupil measurement algorithm

Basic part of the developed system is the algorithm for automatic localization of pupil and calculation of its diameter. This algorithm was based on Kishor Datta Gupta work [26] implemented in C++ to accurately detect and calculate the pupil size. Each frame of the video recording passes through an image processing techniques.

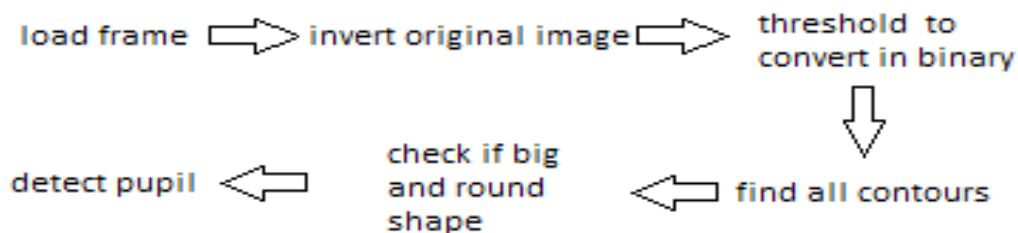


Figure 4.7: Pupil measurement algorithmic steps

Below are listed the results of each step by dividing the whole process into discrete stages.

Firstly the original frame is loaded

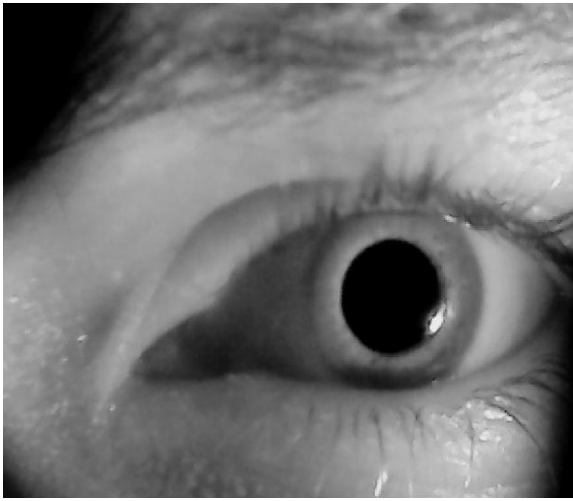


Figure 4.8 (a): original image

Afterward an inversion is applied



Figure 4.8 (b): inverted image

By thresholding the inverted frame a binary image is produced. The threshold value is controlled through the GUI layout in order to eliminate the non-interesting information.



Figure 4.8 (c): binary image

At this point, a set of functions of OpenCV is used to estimate the contours of binary image. Once these contours are found, the algorithm searches which one is large enough and round shaped to refer to the pupil. For each contour found in image a bounding rectangle is determined. Rectangle's width and height could be easily calculated as well as the shape of the contour area through OpenCV functions to

locate the pupil and estimate the diameter. Finally a circle is illustrated on the original image to present the correlation. From the binary image it's obvious that the pupil is not necessarily rounded due to the illumination LEDs. Although the algorithm detects and calculates correctly the pupil size.

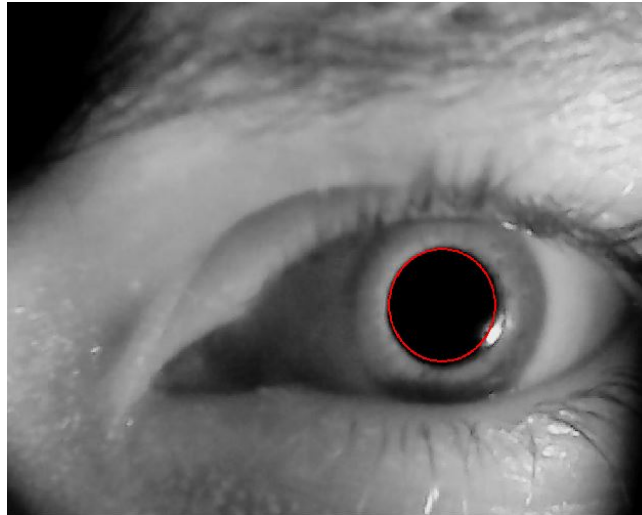
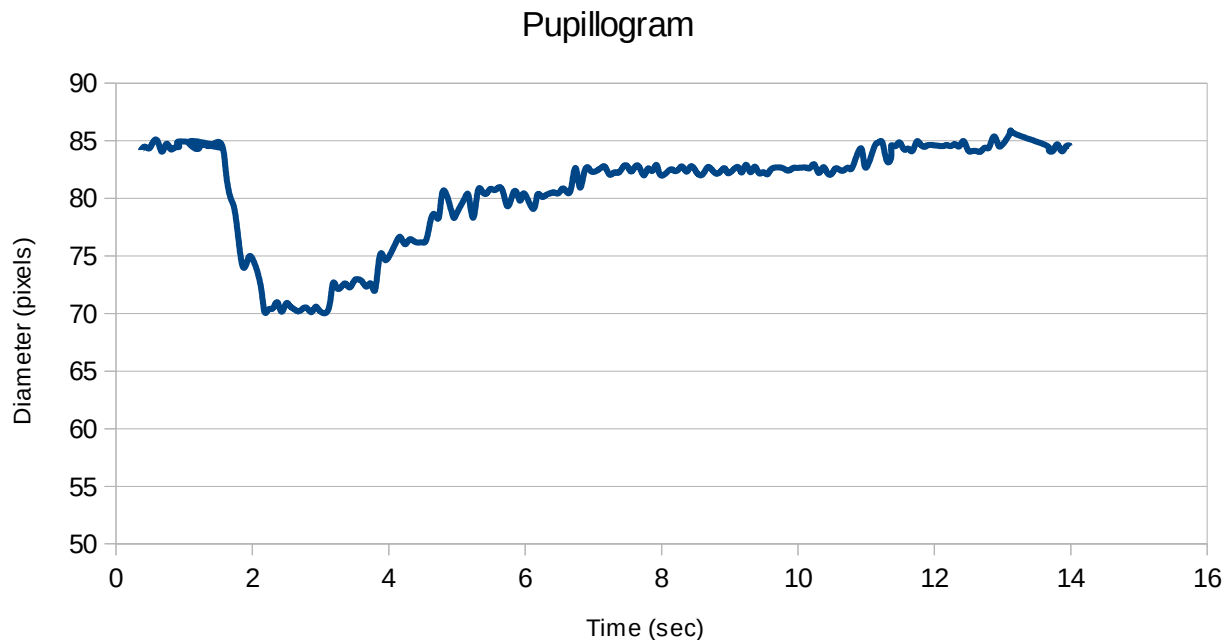


Figure 4.8 (d): Pupil localization image

In conclusion, the algorithmic logic was evaluated by applying the image processing techniques to each frame of the recording within a specific time frame. The form of pupillograms is presented below.



In this example the wait time was set 1.5 seconds, stimulation time for 2 seconds and finally the recovery time for 10 seconds as shown in above diagram.

Conclusion and future work

After completing the theoretical and experimental study of the device, some important conclusions are exported. The use of a pupillometry examination in the field of medicine is considered to be a cost-effective, non-intrusive method of timely diagnosis of a wide variety of pathologies and psychosomatic cases, which can expunge the subjective estimation. The operation of the device in both hardware and software level, is promoted to the skills of a non specialized in engineering user, such as a nurse or a doctor. However, the reaction of the pupil is mainly characterized by significant differences in many circumstances. Thus it is valuable to elicit significant parameters that could determine the behavior of the photomotor reflex. Such parameters can be defined as maximum constriction or dilation, constriction or dilation velocity, total constriction time, pupil recovery time and so on. The next stages of the current research project could involve data analysis on larger and more socio-demographically diverse population samples. In that way, data relating to pathological and non-pathological cases can be separated and linked to a variety of clinical cases. Different pupil reaction from a normalized group may indicate particular diagnosed pathology. In later stages pupillometry may reveal the connection between pupillary reflexes and awareness, cognitive and sentimental condition of a human.

References

- [1] Purves, Dale, George J. Augustine, David Fitzpatrick, William C. Hall, Anthony-Samuel LaMantia, James O. McNamara, and Leonard E. White (2008). *Neuroscience*. 4th ed. Sinauer Associates. pp. 290–1.
- [2] Kerr, R (2016). "Underestimation of pupil size by critical care and neurosurgical nurses". *American J of Critical Care*. 25: 213–219.
- [3] Olson, D (2015). "The use of automated pupillometry in critical care". *Critical Care Nursing Clinics North America*. 28: 101–107.
- [4] Shindler KS, Revere K, Dutt M, Ying G-S, Chung DC, *In Vivo Detection of Experimental Optic Neuritis by Pupillometry*. *Experimental eye research*. 2012;100:1-6.
- [5] Alessio Martucci, Massimo Cesareo, Domenico Napoli, Roberto Pietro Sorge, Federico Ricci, Raffaele Mancino, Carlo Nucci, "Evaluation of pupillary response to light in patients with glaucoma: a study using computerized pupillometry", 2014
- [6] Atsushi Miki, Atsuhiko Iijima, Mineo Takagi, Tomoaki Usui, Shigeru Hasegawa, Haruki Abe, Takehiko Bando "Pupillography of relative afferent pupillary defect contralateral to monocular mature cataract" *Can J Ophthalmol*. 2006 Aug;41(4):469-71
- [7] Hess E. H., Polt J. M. (1960) "Pupil size as related to interest value of visual stimuli" *Science*, 132, 349-350.
- [8] Hess E. H., Seltzer A. L., Shlien J.M. (1965) "Pupil response of hetero- and homosexual males to pictures of men and women: A pilot study" *Journal of Abnormal Psychology*, 70, 165-168
- [9] Simms T. M. (1967) "Pupillary response of male and female subjects to pupillary difference in male and female picture stimuli" *Perception and Psychophysics*, 2, 553-555.
- [10] Fitzgerald H. E. (1968), "Autonomic pupillary reflex activity during early infancy and its relation to social and nonsocial visual stimuli" *Journal of Experimental Child Psychology*, 6, 470-482
- [11] A. Merzouki, J. Molero Mesa, A. Louktibi, M. Kadiri, G.V. Urbano "Assessing changes in pupillary size in Rifian smokers of kif (*Cannabis sativa* L.)" *Journal of Forensic and Legal Medicine* 15, pp. 335–338, 2008

- [12] M. A. Phillips, P. Bitsios, E. Szabadi, C. M. Bradshaw, *Comparison of the antidepressants reboxetine, fluvoxamine and amitriptyline upon spontaneous pupillary fluctuations in healthy human volunteers*, *Psychopharmacology*, 2000, Volume 149, Number 1, Page 72
- [13] Matthias Dutsch, Harald Marthol, Georg Michelson, Bernhard Neundorfer, Max Josef Hilz "Pupillography refines the diagnosis of diabetic autonomic neuropathy" *Journal of the Neurological Sciences* 222 (2004) 75– 81
- [14] A. Keivanidou, D. Fotiou, C. Arnaoutoglou, N. Arnaoutoglou, D. Tsiptsios, D. Partsafyllidis, V. Stergiou, G. Karatasios, A. Karamitrou, A. Karlovasitou, "Changes in pupillary size and mobility in patients with heart failure", *International Journal of Psychophysiology* 69, pp. 242–275, 2008.
- [15] Smith, Shirley A. Dewhirst, Richard R., *A Simple Diagnostic Test for Pupillary Abnormality in Diabetic Autonomic Neuropathy*, *Diabetic Medicine*
- [16] H. Oyamada, A. Iijima, A. Tanaka, K. Ukai, H. Toda, N. Sugita, M. Yoshizawa, T. Bando, "A pilot study on pupillary and cardiovascular changes induced by stereoscopic video movies", *Journal of NeuroEngineering and Rehabilitation*, 2007
- [17] D. Partsafyllidis, D. Fotiou, D. Tsiptsios, A. Keivanidou, V. Stergiou, A. Karamitrou, G. Karatasios, A. Karlovasitou, *Evaluation of pupillary size and mobility in patients with schizophrenia*, In *International Journal of Psychophysiology*, Volume 69, Issue 3, 2008
- [18] V. Stergiou, D. Fotiou, D. Tsiptsios, D. Partsafyllidis, A. Keivanidou, G. Karatasios, A. Karamitrou, A. Karlovasitou, *Pupillometric findings in patients with Parkinson's disease and cognitive disorders*, In *International Journal of Psychophysiology*, Volume 69, Issue 3, 2008
- [19] D.F. Fotiou, V. Stergiou, D. Tsiptsios, C. Lithari, M. Nakou, A. Karlovasitou, *Cholinergic deficiency in Alzheimer's and Parkinson's disease: Evaluation with pupillometry*, In *International Journal of Psychophysiology*, Volume 73, Issue 2, 2009
- [20] D. Tsiptsios, D. Fotiou, V. Stergiou, D. Partsafyllidis, A. Keivanidou, A. Karlovasitou, *Evaluation of pupillary size and mobility in patients with Myasthenia Gravis*, In *International Journal of Psychophysiology*, Volume 69, Issue 3, 2008
- [21] Xiaofei Fan "Abnormal Transient Pupillary Light Reflex in Individuals with Autism Spectrum Disorders" *J Autism Dev Disord.* 2009 November

- [22] Grünberger J, Linzmayer L, Grunberger M, *Pupillometry in clinical psychophysiological diagnostics: methodology and proposals for application in psychiatry*, *Isr J Psychiatry Relat Sci* 1992
- [23] Adriana L. Bertrand, João Batista Santos Garcia, Erica B. Viera, Alcione M. Santos, and Romero H. Bertrand “The Influence of Gender and Anxiety on the Pain Response” *European Journal of Pain*, 2013
- [24] Hidetoshi Mori, Shoichi Ueda, Hiroshi Kuge, Eiichi Taniwaki, Tim Hideaki Tanaka, Kiyoshi Adachi, Kazushi Nishijo, "Pupillary response induced by acupuncture stimulation – an experimental study", *Acupuncture in Medicine* 26(2), 2008
- [25] Akino Wakasugi, Hiroshi Odaguchi, Tetsuro Oikawa, Toshihiko Hanawa, "Effects of goshuyuto on lateralization of pupillary dynamics in headache", *Autonomic Neuroscience: Basic and Clinical* 139, pp. 9–14, 2008.
- [26] Kishor Datta Gupta, *Pupil or eyeball detection and extraction from eye image using C#*, Research assistant of University of Memphis
- [27] Paraskevi Dretaki "Study of pupil response to multiwavelength excitation in normal and pathologic conditions", *Diploma Thesis*
- [28] Vasileios Kavvadias “Imaging System for the pupillary photomotor reflex meter analysis”, *Diploma Thesis*